# Design, Synthesis, and in Vitro and in Vivo Evaluation of Ouabain Analogues as Potent and Selective Na,K-ATPase α4 Isoform Inhibitors for Male Contraception

Shameem Sultana Syeda,[†] Gladis Sánchez,[‡] Kwon Ho Hong,[†] Jon E. Hawkinson,[†] Gunda I. Georg,*,[†] and Gustavo Blanco*,[‡]

[†]Department of Medicinal Chemistry and Institute for Therapeutics Discovery and Development, College of Pharmacy, University of Minnesota, Minneapolis, Minnesota 55414, United States

[‡]Department of Molecular and Integrative Physiology, University of Kansas Medical Center, Kansas City, Kansas 66160, United States

S *Supporting Information*
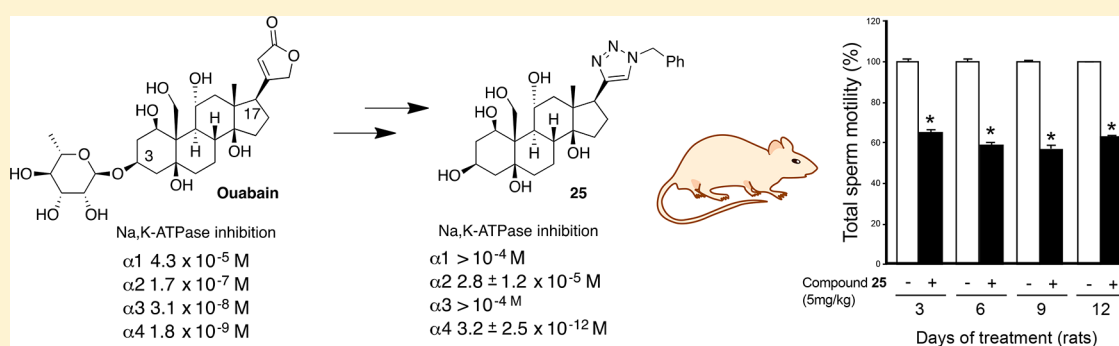
ABSTRACT: Na,K-ATPase α4 is a testis-specific plasma membrane Na^+ and K^+ transporter expressed in sperm flagellum. Deletion of Na,K-ATPase α4 in male mice results in complete infertility, making it an attractive target for male contraception. Na,K-ATPase α4 is characterized by a high affinity for the cardiac glycoside ouabain. With the goal of discovering selective inhibitors of the Na,K-ATPase α4 and of sperm function, ouabain derivatives were modified at the glycone (C3) and the lactone (C17) domains. Ouabagenin analogue **25**, carrying a benzyltriazole moiety at C17, is a picomolar inhibitor of Na,K-ATPase α4, with an outstanding α4 isoform selectivity profile. Moreover, compound **25** decreased sperm motility in vitro and in vivo and affected sperm membrane potential, intracellular Ca^{2+}, pH, and hypermotility. These results proved that the new ouabagenin triazole analogue is an effective and selective inhibitor of Na,K-ATPase α4 and sperm function.

■ INTRODUCTION

Unintended pregnancies have been on the rise in the past years, and their management represents a priority and a challenge for any public health program.[1−3] Many of these pregnancies end in elective abortions and are frequently associated with physical and emotional complications and high economical costs.[4,5] It is clear that developing safe, effective, and reversible methods of contraception are needed to enhance birth control options. Currently, several contraceptive methods are available for women, including hormonal treatment, intrauterine devices, and implants. These approaches place a disproportionate responsibility for birth control on women and the potential risk for complications.[6−8] It is clear that a more comprehensive and sustainable family planning program requires extending contraception to males.[9] However, male contraceptive methods are basically limited to the use of condoms and vasectomy.[10] A safe, effective, and reversible contraceptive for men is still unavailable.[11,12]

An attractive approach to develop a male contraceptive is the targeting of proteins that are essential for sperm fertility.[13,14] The finding that some proteins are specifically expressed in sperm provides the additional opportunity to interfere with male fertility, minimizing other toxic side effects.[15−18] Evidence from our laboratory has shown that Na,K-ATPase α4 is an attractive target for male contraception.[19,20] Na,K-ATPase is an active ion transport system of the cell plasma membrane, which utilizes the energy from the hydrolysis of ATP to exchange intracellular Na^+ for extracellular K^+.[21] Structurally, Na,K-ATPase is a heterodimeric molecular complex, constituted by α and β subunits.[22] The α subunit, considered the catalytic subunit of the enzyme, is a multipass transmembrane protein of 110−112 kDa, which contains the binding sites for ATP, Na^+, K^+, and the cardiotonic inhibitor ouabain.[23] The β peptide is a 40−60 kDa single membrane spanning protein, which plays an
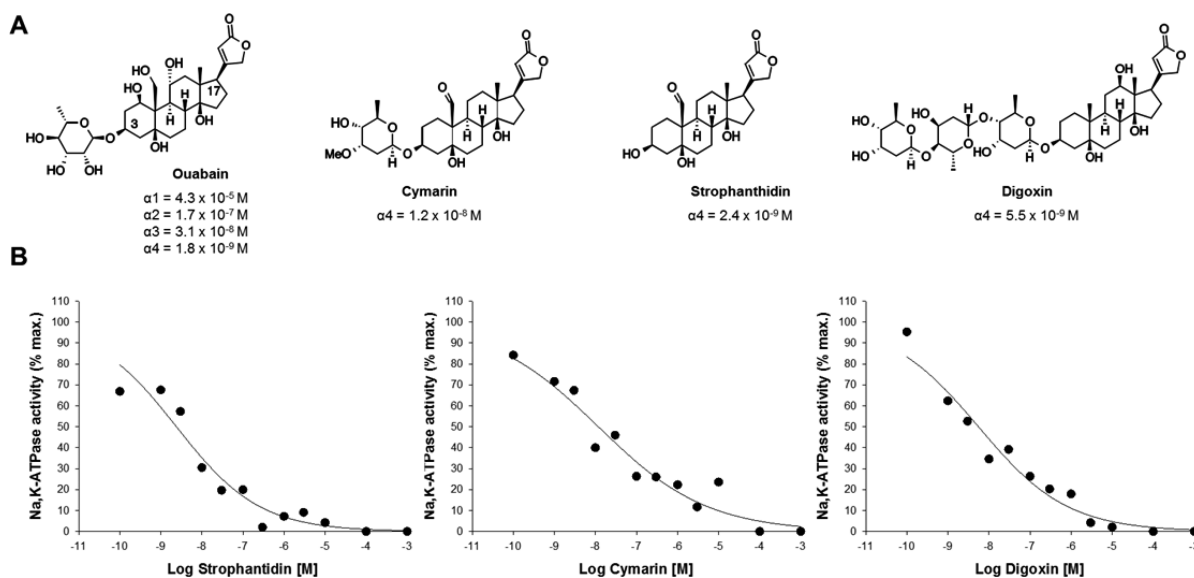
Figure 1. (A) Structures of ouabain, strophanthidin, cymarin, and digoxin and their IC$_{50}$ values for Na,K-ATPase isoform inhibition. IC$_{50}$ values for ouabain are taken from ref 35. (B) Dose−response curves for the inhibition of Na,K-ATPase α4 activity by strophanthidin, cymarin, and digoxin. Values are the mean of two experiments performed in quadruplicate.

important role in the folding, stability, and targeting of the α subunit to the plasma membrane.[24] Several genes, encoding a family of α (α1, α2, α3, and α4) and β (β1, β2, and β3) peptides, have been identified in mammals.[25,26] Both α and β subunits are expressed in different combinations, in a cell type-specific and developmentally regulated manner.[27] Each Na,K-ATPase αβ pair has different functional characteristics with respect to their affinities for ions, ATP, and ligands. Na,K-ATPase functional properties mainly depend on the α subunit composition of the transporter, with each α isoform exhibiting distinct functional characteristics.[28] The α4 isoform is the Na,K-ATPase isoform with the most restricted pattern of expression, being uniquely present in male germ cells of the testis.[29] Its expression is up-regulated at postmeiotic stages of spermatogenesis, becoming abundant in the sperm flagellum.[30,31] The activity of Na,K-ATPase α4 is essential for maintaining sperm intracellular Na$^+$ levels ([Na$^+$]$_i$) and for the control of several other vital sperm parameters including membrane potential (V_m), intracellular Ca^{2+} ([Ca^{2+}]$_i$), and pH.[32] Importantly, Na,K-ATPase α4 is crucial for sperm motility and sperm hyperactivation, a key event associated with sperm capacitation.[33,34] Additional information on the role of Na,K-ATPase α4 in male fertility was obtained through experiments in genetically modified mice, in which this particular ion transporter was deleted. The Na,K-ATPase α4 knockout mice are overall phenotypically normal, and their testes are indistinguishable in size and morphology from those of wild-type mice. Also, male mice lacking Na,K-ATPase α4 are able to produce normal sperm numbers. However, the male mice are completely infertile due to defects in sperm morphology, motility, and hyperactivation. In contrast, female mice from the Na,K-ATPase α4 null colony are fertile.[19,30] This shows that, while α4 is not needed for sperm production, it is an absolute requirement for male fertility. In addition, this provides strong evidence for the suitability of Na,K-ATPase α4 as a pharmacological target for the control of male fertility.

From a biochemical standpoint, Na,K-ATPase α4 has functional characteristics that are highly unique and different from those of the other Na,K-ATPase isoforms. Compared to Na,K-ATPase α1, α2, and α3 isoforms, α4 has a relatively higher apparent affinity for Na$^+$, a lower apparent affinity for K$^+$, and an intermediate affinity for ATP.[35] In addition, Na,K-ATPase α4 is less sensitive to voltage.[36]

The Na,K-ATPase is a receptor for cardenolides and cardiac glycosides. The cardenolides are a family of compounds that consist of a steroidal nucleus or aglycone and a five-membered unsaturated lactone ring attached at C17 of the steroid backbone. Cardenolides that contain a specific sugar moiety attached at C3 of the aglycone are known as cardiac glycosides. Ouabain is a cardiac glycoside that can be isolated from *Strophanthus gratus* and *Acokanthera schimperi*. It is used extensively in biomedical research and has been used for the therapy of heart attacks and for the treatment of patients with left ventricular insufficiency.[37] Ouabain is an endogenous steroidal hormone of mammals that is synthesized in the adrenal glands and the hypothalamus.[38,39] An intriguing characteristic of the Na,K-ATPase α4 isoform is its high affinity for several cardiac glycosides, including ouabain (Figure 1).

According to our results, ouabain has an IC$_{50}$ value in the low nanomolar range for Na,K-ATPase α4, and it is 10 000-fold selective for Na,K-ATPase α4 over the ubiquitously expressed Na,K-ATPase α1 isoform, which is the only other Na,K-ATPase present in sperm.[35] These values correspond to the Na,K-ATPase of rat, in which the α1 isoform also has a low affinity for ouabain. In humans, the ouabain affinity for Na,K-ATPase α4 is also high and similar to that of rat, but because the human Na,K-ATPase α1 has a higher sensitivity to ouabain than in rat,[40] the difference in ouabain affinity between human Na,K-ATPase α1 and α4 isoforms is narrower. Despite this, human Na,K-ATPase α4 is ~100-fold more sensitive to ouabain than α1.[35] This distinct sensitivity for ouabain has been used as a tool to selectively inhibit Na,K-ATPase α4 and explore its physiological relevance, independently from that of α1 and other Na,K-ATPase isoforms. Thus, blocking Na,K-ATPase α4 with relatively low concentrations of ouabain provided the first evidence as to the role of this isoform in sperm motility. The preferential inhibition of Na,K-ATPase α4 with ouabain impairs the sperm total motility and multiple parameters of sperm

movement, including progressive motility, straight line, curvilinear and average path velocities, lateral head displacement, beat cross frequency, and linearity, both in rat and human sperm.[32,40] The use of higher ouabain concentrations that also inhibited Na,K-ATPase α1 did not cause additional reduction in sperm motility.[32,34] These results showed the specific role that Na,K-ATPase α4 has in sustaining multiple aspects of sperm flagellar movement. Additional evidence for the effect of ouabain on male fertility comes from a clinical study suggesting a possible correlation between endogenous ouabain levels and reduced fertility in humans. Patients with high endogenous ouabain levels in seminal plasma (26.52 ± 1.82 μg/L) displayed severe asthenozoospermia compared to normal fertile subjects, who have lower levels of ouabain in semen (19.31 ± 1.45 μg/L).[41]

Taken together, these results suggest that ouabain is an attractive chemical scaffold to develop compounds that can specifically target Na,K-ATPase α4. Since ouabain itself exerts toxic effects in the heart, new compounds with greater isoform specificity toward α4 are needed for the development of safe male contraceptives. Here, we describe a new ouabagenin triazole analogue, which is an effective and selective inhibitor of Na,K-ATPase α4 and sperm function.

■ RESULTS

First, we tested cardiac glycoside containing carbohydrate moieties of different lengths, including cymarin and digoxin and the cardenolide strophanthidin (Figure 1). We examined their capacity to inhibit the enzymatic function of Na,K-ATPase α4 by measuring the Na$^+$, K$^+$, and Mg^{2+} dependent hydrolysis of ATP that is sensitive to ouabain. As the source of the enzyme, we prepared recombinant rat Na,K-ATPase α4 by expression in Sf9 insect cells using baculoviruses as described previously.[35] This expression system has been extensively used in the past to study Na,K-ATPases. It provides the advantage that Sf9 insect cells have no endogenous Na,K-ATPase; therefore, activity of the expressed foreign protein can be studied in an environment free of any contaminating Na,K-ATPase.[42] We infected Sf9 cells with baculoviruses that direct the expression of the Na,K-ATPase α4 and β1 subunits. Whole lysates from the cells were used, and the Na,K-ATPase activity under saturating amounts of Na$^+$, K$^+$, and ATP was measured as previously described.[43] The results showed that strophanthidin (without a sugar moiety attached at 3-OH), cymarin (one sugar moiety attached at 3-OH), and digoxin (three sugar rings attached to 3-OH) inhibited Na,K-ATPase α4 with similar IC$_{50}$ values (10^{-8} to 10^{-9} M) compared to ouabain. This indicated that the sugar moiety in cardiac glycoside is a structural feature that does not significantly influence binding of the compounds to the Na,K-ATPase α4 isoform.

On the basis of these results and the well-known fact that the C17 substituent is an important moiety for binding to Na,K-ATPase,[44] which forms a hydrogen bond with the receptor,[45] we designed and synthesized new ouabain analogues in which the aglycone (C3) and the lactone ring (C17) domains were modified. We investigated the 1,2,3-triazole moiety as a replacement for the lactone moiety.[46] This replacement seemed promising as triazoles can function as hydrogen bond acceptors, and in addition, can engage in dipole and π–π interactions.[47] We prepared triazole analogues in which the steroidal moiety was directly connected to a triazole or linked via a methylene or a hydroxymethylene spacer (Figure 2). Our efforts to modify the C17 domain also included the replacement of the 5-

Figure 2. Design of ouabain analogues.

membered α,β-unsaturated butyrolactone ring of ouabain with hydroxymethyl, oxime, nitrile, and acid groups. These analogues could be easily prepared from intermediates generated during the synthesis of the triazole analogues. As we show in the present work, the synthetic ouabain derivatives that we have generated inhibit Na,K-ATPase α4 and affect sperm motility, both in vitro and in vivo after oral administration to rats.
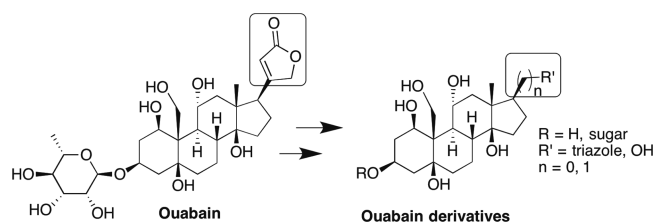
The syntheses of the ouabain analogues are shown in Schemes 1−5. As depicted in Scheme 1, commercially available ouabain was converted into the corresponding diacetonide 1,[48] followed by protection of the hydroxyl groups of 1 with methoxymethyl chloride and diisopropylethylamine (MOM-Cl/DIPEA) to yield intermediate 2 in 68%. Ozonolysis of the lactone olefin in compound 2 followed by hydrolysis of the resulting ester provided an unstable hydroxymethyl ketone. The crude hydroxymethyl ketone was subsequently reduced with NaBH$_4$ to form a diastereomeric mixture of diols 3 in 42% yield over three steps, which were subsequently subjected to oxidative cleavage with NaIO$_4$ to furnish aldehyde 4. Treatment of aldehyde 4 with ethynylmagnesium bromide generated alkynols 5 as an inseparable diastereomeric mixture (3:1 ratio). Next, the alkynes 5 were subjected to 1,3-cycloaddition with the respective azides (benzyl and 4-fluorobenzyl azides) using click reaction conditions to form triazoles 6 and 7. Exposure of 6 and 7 to 4 N HCl in MeOH resulted in the removal of the acetonide and MOM groups to yield triazoles 8 and 9 in 42% and 40% yields, respectively.

The C17 hydroxymethyl analogue 10 and the nitrile analogue 11 were prepared from aldehyde 4 by reduction of the aldehyde and nitrile formation, respectively, as shown in Scheme 2. Attempts for the global deprotection (acetonide and MOM-ethers) of these compounds were unsuccessful.

Scheme 3 describes the synthesis of ouabain analogues with modifications at the C3 and C17 positions. The synthesis began by simultaneously removing the sugar and introducing the acetonide protecting group with HCl in acetone to generate ouabagenin monoacetonide 12[49] in 55% yield. Intermediate 12 was transformed to aldehyde 16 in an analogous manner to that described in Scheme 1 (conversion of 2 to 4). The three hydroxyl groups of intermediate 12 were protected as MOM ethers to obtain 13 in 75% yield. Ozonolysis of 13 followed by hydrolysis of the resulting ester provided the unstable hydroxymethyl ketone 14 in 63% yield over two steps. Reduction of 14 followed by oxidative cleavage of the resulting diols 15 with NaIO$_4$ provided aldehyde 16 in 62% yield. Reduction of aldehyde 16 with NaBH$_4$ in MeOH furnished alcohol 17 in 72% yield, which was converted to the corresponding tosylate in 73% yield. Nucleophilic displacement of the tosylate group with NaN$_3$ in DMF provided azide 18 in 70% yield. Click reaction between azide 18 and 4-methoxyphenyl acetylene provided the corresponding triazole

Scheme 1. Synthesis of C17 Hydroxymethylene Triazole Analogues[a]
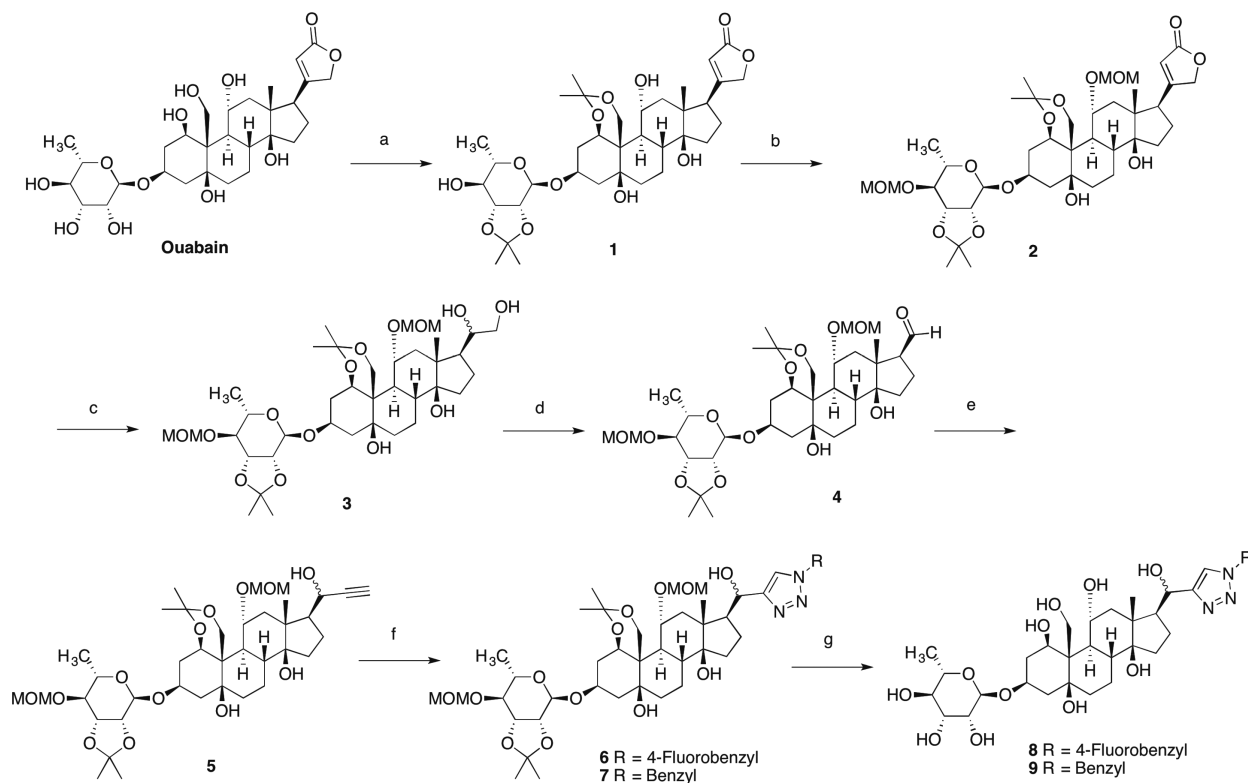
[a]Reagents and conditions: (a) acetone, concentrated HCl, rt, 84%; (b) MOM-Cl, DIPEA, CH_2Cl_2, rt, 68%; (c) (i) O_3, −78 °C then Zn/AcOH, CH_2Cl_2, (ii) $KHCO_3$, MeOH, rt, (iii) $NaBH_4$, MeOH, 42% (for 3 steps); (d) $NaIO_4$, THF/H_2O (8:2), rt, 63%; (e) ethynylmagnesium bromide, THF, −78 °C, 74%; (f) benzyl azide or 4-fluorobenzyl azide, Cu_2SO_4·$5H_2O$ (20 mol %), sodium ascorbate (40 mol %), DMF/H_2O, **6** (40%), **7** (64%); (g) 4 N HCl in MeOH, rt, **8** (42%), **9** (40%).

Scheme 2. Synthesis of C17 Hydroxymethyl and Nitrile Analogues[a]
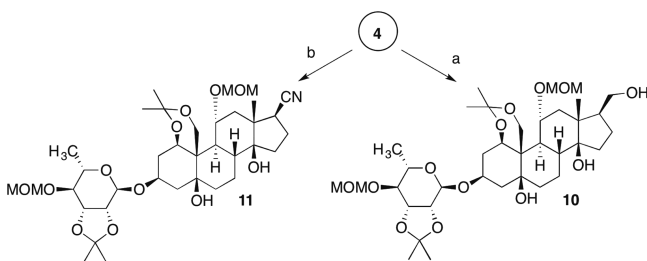
[a]Reagents and conditions: (a) $NaBH_4$, MeOH, 78%; (b) (i) NH_2OH·HCl, NaOAc, (ii) CDI, CH_2Cl_2, 70% (for 2 steps).

derivative, which was deprotected with 4 N HCl in MeOH to yield the target compound **19** in 51% yield.

The synthesis of ouabain analogues in which the triazole moiety is directly attached to C17 was accomplished as shown in Scheme 4. Aldehyde **16** upon reaction with the Bestmann–Ohira reagent **20** (dimethyl(1-diazo-2-oxopropyl)-phosphonate) furnished alkyne **21** in 71% yield. The triazole ring was installed by click chemistry between alkyne **21** and benzyl azide, 4-chlorobenzyl azide, and 4-fluorobenzyl azide in 58%, 56%, and 66% yields, respectively. ^{1}H NMR analysis revealed the formation of triazole diastereomers, indicating that partial epimerization occurred at the C17 position during the introduction of the alkyne. The major diastereomers of triazoles **22** and **23** could be separated by multiple flash column chromatography.[50] Diastereomerically pure intermediates **22**

and **23** and the diastereomeric mixture **24** were deprotected with 4 N HCl to provide target compounds **25** and **26** as single isomers and **27** as a diastereomeric mixture.
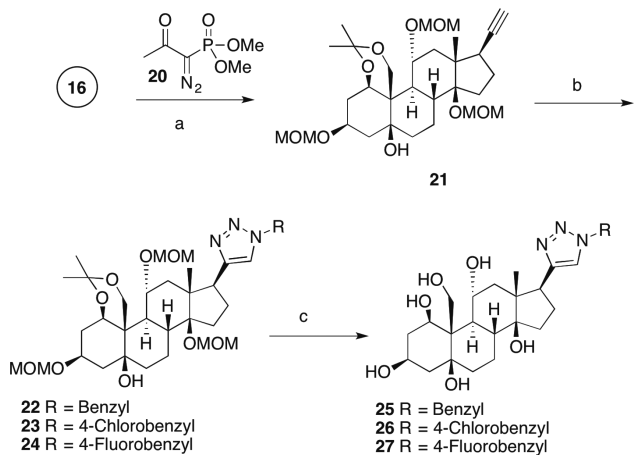
Scheme 5 shows the synthesis of additional ouabain analogues that were readily accessible from aldehyde **16**. Aldehyde **16** was converted to oxime **28** in 81% yield by reaction with hydroxylamine and then dehydrated to furnish nitrile **29** in 78% yield. Reaction of aldehyde **16** with $TMSCF_3$ provided trifluoroethanol analogue **30**. The propynyl analogue **31** was obtained by reaction of aldehyde **16** with ethynylmagnesium bromide in 79% yield. Oxidation of hydroxyethanone intermediate **14** provided the C17 acid analogue **32** in 52% yield.

Activity of Ouabain Analogues As Inhibitors of Na,K-ATPase α4. The activity of the synthetic ouabain analogues was examined as reported previously,[43] using recombinant Na,K-ATPase α4 and β1 subunits expressed in insect cells. Ouabain analogues inhibited the activity of Na,K-ATPase α4 with a broad range of potencies, from 10^{-5} to 10^{-12} M (Table 1).

Of the 19 compounds tested, most retained significant inhibitory activity. The most potent inhibitors were analogues **25**, **17**, and **10**. These three compounds are differently substituted at C3. Compound **10** carries a protected carbohydrate, compound **17** a methoxymethyl protecting group, and analogue **25** a hydroxyl group, supporting the finding from testing the cardenolides (Figure 1) that the C3 carbohydrate group is not required for activity and furthermore indicating that this site can tolerate a variety of groups without

Scheme 3. Synthesis of C3 and C17 Modified Triazolylmethyl Analogues[a]
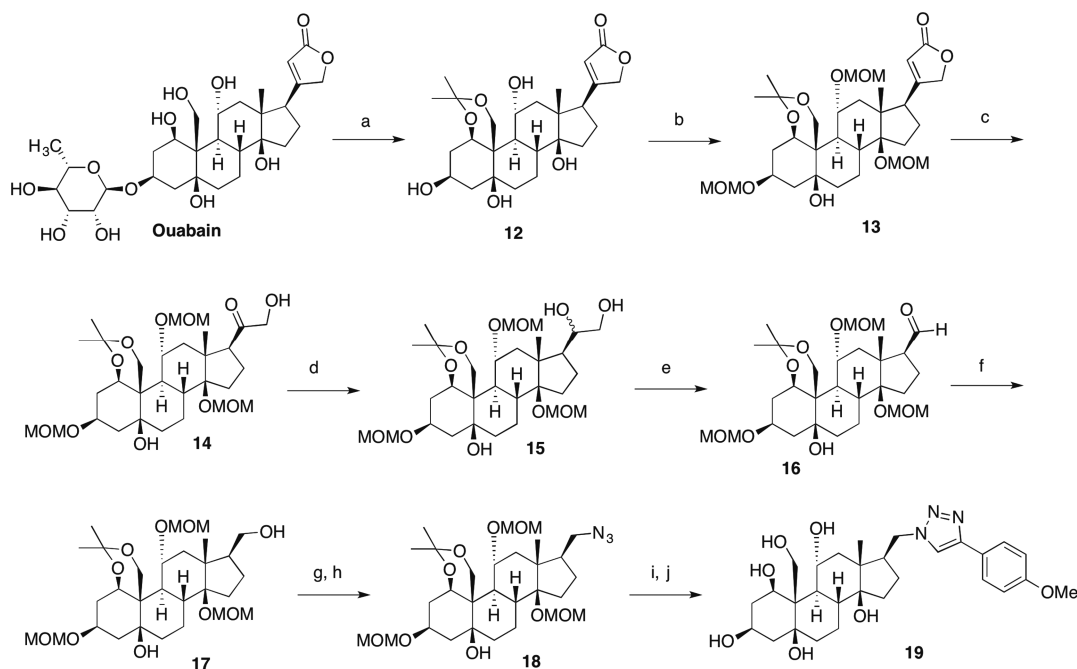
[a]Reagents and conditions: (a) acetone, concentrated HCl, rt, 55%; (b) MOM-Cl, DIPEA, rt, 75%; (c) (i) O$_3$, −78 °C then Zn/AcOH, CH$_2$Cl$_2$, (ii) KHCO$_3$, MeOH, rt, 63% (for 2 steps); (d) NaBH$_4$, MeOH, 76%; (e) NaIO$_4$, THF/H$_2$O (8:2), rt, 62%; (f) NaBH$_4$, MeOH, 72%; (g) TsCl, pyridine, 73%; (h) NaN$_3$, DMSO, 60 °C, 70%, (i) 4-methoxyphenyl acetylene, Cu$_2$SO$_4$·5H$_2$O (20 mol %), sodium ascorbate (40 mol %), DMF/H$_2$O, 68%; (j) 4 N HCl in MeOH, rt, 51%.

Scheme 4. Synthesis of C17 Triazole Analogues[a]

22 R = Benzyl
23 R = 4-Chlorobenzyl
24 R = 4-Fluorobenzyl

25 R = Benzyl
26 R = 4-Chlorobenzyl
27 R = 4-Fluorobenzyl

[a]Reagents and conditions: (a) K$_2$CO$_3$, MeOH, 71%; (b) benzyl azide (22, 58%), 4-chlorobenzyl azide (23, 56%), or 4-fluorobenzyl azide (24, 66%), Cu$_2$SO$_4$·5H$_2$O (20 mol %), sodium ascorbate (40 mol %), DMF/H$_2$O; (h) 4 N HCl in MeOH, rt, 25 (47%), 26 (51%), 27 (53%).

Scheme 5. Synthesis of C17 Substituted Analogues[a]
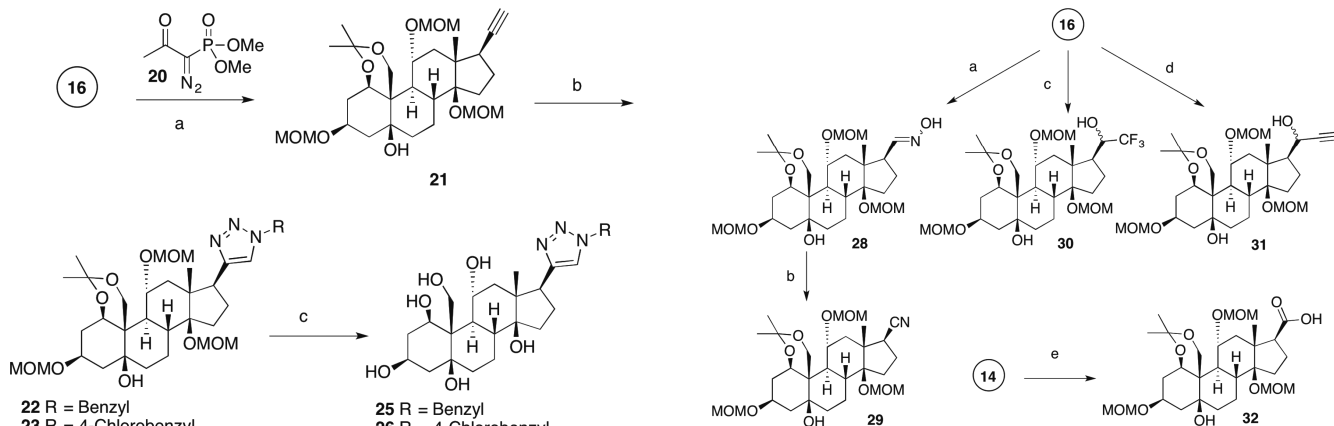
[a]Reagents and conditions: (a) NH$_2$OH·HCl, NaOAc, EtOH, rt, 81%; (b) CDI, CH$_2$Cl$_2$, rt, 78%; (c) TMSCF$_3$, TBAF, THF, rt, 46%; (d) ethynylmagnesium bromide, THF, −78 °C, 79%; (e) NaIO$_4$, H$_2$O/AcOH (2:1), EtOH, rt, 52%.

reduction in potency. Compound **25** is a picomolar inhibitor, carrying a C17 *N*-benzyltriazole moiety that we introduced as a replacement of the cardenolide C17 lactone. The introduction of this group enhanced potency significantly, and as will be shown below, the selectivity was enhanced substantially as well (Table 2). The 4-chloro- and 4-fluoro-benzyl analogues **26** and **27** were significantly less potent than **25**, indicating that substitution is unfavorable at that position, but they were still 30 nM inhibitors. Compounds **10** and **17** that carry a C17 hydroxymethyl group are nanomolar and subnanomolar

inhibitors, respectively, demonstrating that this group effectively replaced the lactone and furthermore conferred excellent selectivity for the inhibition of the α4-isoform (Table 2). The outstanding inhibitory properties of compounds **10** and **17** was surprising because they both carry acetonide and methoxymethyl protecting groups, indicating that modifications at the C1, C19, C11, and C14 hydroxyl groups unexpectedly did not negatively influence the inhibitory effectiveness of these compounds. Other potent analogues are the C17 aldehyde **4** and the C17 oxime **28**, which have potencies similar to ouabain. Although a range of C17 modifications could be made at C17 without a loss of inhibitory activity, other C17 modifications

**Table 1. IC$_{50}$ Values for the Inhibition of Na,K-ATPase α4 Activity by Ouabain Analogues**

compound	IC$_{50}$ (M)^a
ouabain	4.3, 8.5 × 10^{-9}
1	4.0, 4.3 × 10^{-9}
3	2.1, 3.7 × 10^{-6}
4	4.9, 7.1 × 10^{-9}
6	1.2, 7.0 × 10^{-8}
8	1.3, 4.4 × 10^{-8}
9	1.2, 1.5 × 10^{-6}
10	0.6, 1.6 × 10^{-9}
11	3.3, 6.2 × 10^{-8}
17	1.1, 1.8 × 10^{-11}
19	1.5, 3.9 × 10^{-5}
22	5.0, 6.9 × 10^{-9}
25	1.7, 3.2 × 10^{-12}
26	3.2, 4.3 × 10^{-8}
27	3.2, 4.9 × 10^{-8}
28	1.4, 2.9 × 10^{-9}
29	1.6, 3.7 × 10^{-5}
30	5.6, 5.9 × 10^{-6}
31	1.0, 6.0 × 10^{-8}
32	3.9, 7.7 × 10^{-8}

^{a}IC$_{50}$ values were calculated from dose−response curves for inhibition of Na,K-ATPase α4β1 expressed in Sf9 insect cells. The values shown are the results of the best fit of the data obtained from two independent experiments.

did lead to reduced activity. The C17 modified hydroxymethyl spacer analogues with and without C3 modifications (**3**, **9**, and **30**) showed a significant decrease in activity, except compounds **6**, **8** and **31**, which displayed double-digit nanomolar activities. The C17 modified nitrile **11** and the C17 carboxylic acid analogue **32** showed about 10-fold reduced activity compared to ouabain. The comparison between C17 carboxylic acid analogue **32** and the corresponding nitrile analogue **29** demonstrated that the introduction of the nitrile moiety reduced activity by 3 orders of magnitude. Similarly, a comparison between the picomolar inhibitor **25** and the corresponding methylene bridged triazole analogue **19** led to a 7 orders of magnitude loss of activity. On the basis of these results, we selected compounds **10**, **17**, and **25** for further study because they exhibited a high inhibitory activity for Na,K-ATPase α4.

Due to their high inhibitory activity, we tested whether compounds **10**, **17**, and **25** had a preferential effect on the Na,K-ATPase α4 isoform by measuring their inhibitory activity against the other Na,K-ATPase isoforms (α1, α2, and α3), also obtained after expression in Sf9 cells. As shown in Figure 3A−C, the ouabain analogues exhibited a much weaker inhibitory activity against the Na,K-ATPase α1, α2, and α3 isoforms than against Na,K-ATPase α4.

In order to obtain insight concerning the binding mode of ouabain and its analogues in the binding pocket, we constructed homology models of the rat α1 and α4 isoforms of Na,K-ATPase using Prime[51] on the basis of the cocrystal structure of the shark-derived Na,K-ATPase with ouabain (PDB ID: 3A3Y).[45,52] The identities between the Na,K-ATPase of the shark renal gland (uniprot ID: Q4H132) and the human and rat α4 isoforms (uniprot IDs: Q13733 and Q64541, respectively) are 75% and 74%, respectively. The final homology models were generated via the relaxation of the initial models without ouabain using MacroModel,[53] followed by the incorporation of ouabain and protein preparation with the protein preparation wizard in the Schrodinger Suite.[54] Initially, we performed molecular docking studies and compared the docking poses of ouabain and analogue **25** in the Na,K-ATPase α1 and α4 isoforms (Supporting Information, Figure 1). The static docking models did not show preferential binding of ouabain and **25** to the α4 isoform. We, therefore, performed molecular dynamics (MD) simulations, which can offer information about relative binding affinities of a ligand and enzyme isoforms.[55] As shown in Figure 4A, Na,K-ATPase α4 and ouabain form direct H-bonds between Asn129 and 19-OH and Thr804 with 14-OH. The same amino acids, Asp129 and Thr804, of the rat α1 isoform form water-mediated H-bonds with ouabain. Thr804 is a crucial amino acid residue for ouabain binding (Thr797 in the reference).[56] Thr804 of the rat α1 interacts with ouabain with lower frequencies than those of the rat α4 isoform. This suggested that these interactions might be important for ouabain's selectivity for the rat α4 isoform over the rat α1 isoform. With respect to compound **25**, the 1-OH, 11-OH, and 19-OH groups maintain direct hydrogen bonding interactions with Asn129 and His118 of the rat α4 isoform with higher frequencies compared to the corresponding amino acid residues Asp129 and Arg118 of the rat α1 isoform (Figure 4C,D). These might be the key interactions for the selectivity of **25** for the rat α4 over the rat α1 isoform. An

Table 2. Structures of Compounds 10, 17, and 25 and Their IC$_{50}$ Values for the Inhibition of Different Na,K-ATPase Isoforms
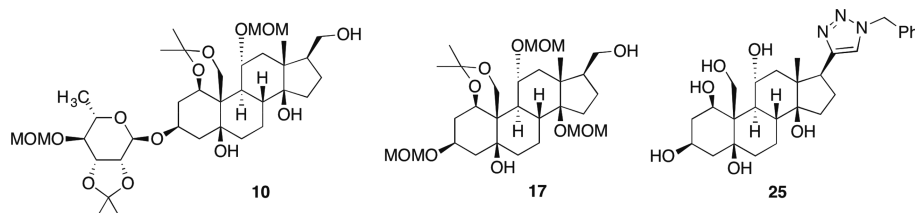
compound	isoform specificity of cardenolides IC$_{50}$ (M)^a			
	α4	α1	α2	α3
10	1.6 ± 0.5 × 10^{-9}	>10^{-4}	>10^{-4}	>10^{-4}
17	1.1 ± 0.6 × 10^{-11}	>10^{-4}	6.6 ± 2.4 × 10^{-6}	>10^{-4}
25	3.2 ± 2.5 × 10^{-12}	>10^{-4}	2.8 ± 1.2 × 10^{-5}	>10^{-4}

^{a}The IC$_{50}$ values were calculated from dose−response curves of inhibition of Na,K-ATPase α1β1, α2β1, α3β1, and α4β1 expressed in Sf9 insect cells. Values are the mean ± SEM of three independent experiments.
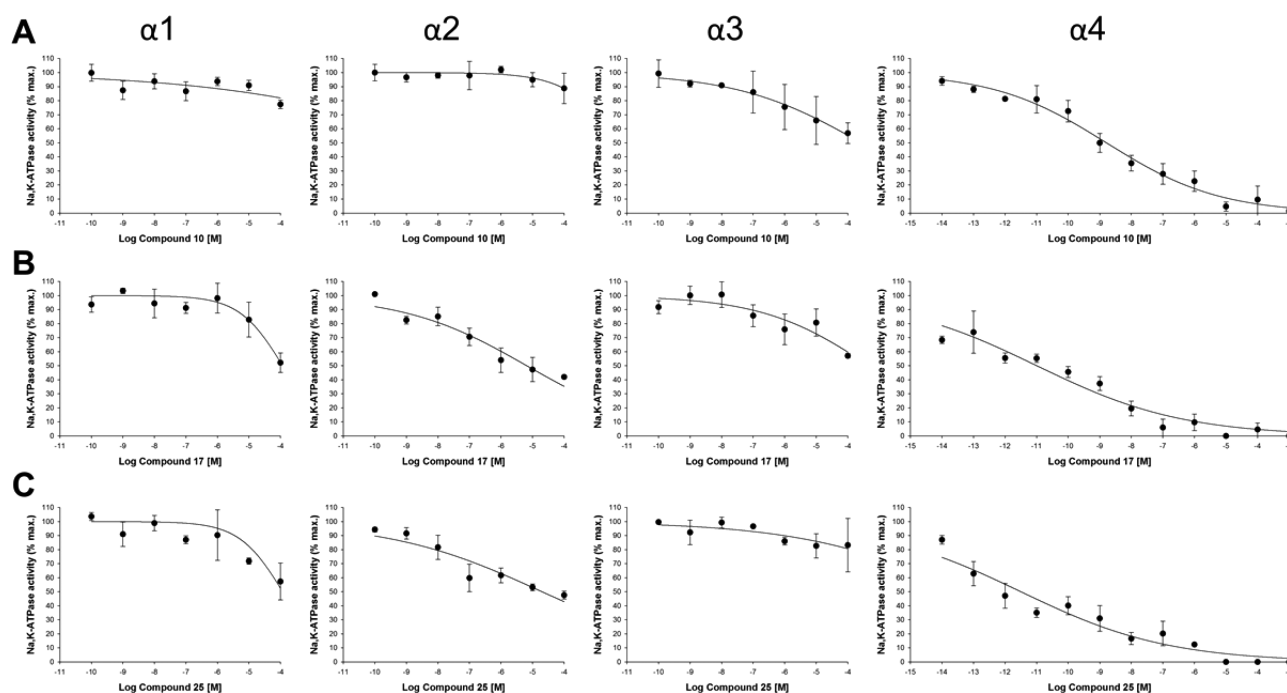
Figure 3. Selectivity of ouabain analogues on Na,K-ATPase $\alpha4$ over other isoforms. Dose−response curves for the inhibition of Na,K-ATPase activity by compounds **10** (A), **17** (B), and **25** (C) were determined on rat $\alpha1\beta1$, $\alpha2\beta1$, and $\alpha3\beta1$ produced in Sf9 insect cells and were compared to that of $\alpha4\beta1$. Hydrolysis of ATP in the presence of saturating concentrations of Na$^+$, K$^+$, and Mg^{2+} was measured using $\gamma[^{32}P]$-ATP. The curves represent the best fit of the experimental data, assuming a single population of binding sites. Each value is the mean $\pm$ SEM of three independent experiments. The corresponding IC$_{50}$ values are shown in Table 2 and exhibit a much lower affinity, in the micromolar and millimolar range for Na,K-ATPases $\alpha1$, $\alpha2$, and $\alpha3$, compared to the nanomolar to picomolar range observed for Na,K-ATPase $\alpha4$.

additional stabilizing effect is the interaction of **25** with Arg887 of the rat $\alpha4$ isoform compensating for the loss of the hydrogen bonding interaction with Thr804. The simulation results are consistent with the results from the Na,K-ATPase inhibition assay, suggesting that the homology model could serve as a tool for the design of additional ouabain analogues.

To determine the effect of compounds **10**, **17**, and **25** more directly on sperm function, we tested their capacity to affect rat sperm motility in vitro. Sperm were isolated from the cauda epididymis of rats and incubated in the absence and presence of **10**, **17**, and **25** for 1 h, and then sperm motility was determined using computer-assisted sperm analysis (CASA). Compounds **10**, **17**, and **25** reduced total sperm motility (Figure 5A). In agreement with their IC$_{50}$ values for inhibition of Na,K-ATPase $\alpha4$ activity, **25** displayed the largest reduction in sperm motility, decreasing sperm motility by approximately 60% at concentrations of 10^{-8} M and higher (Figure 5A). The activity of the compounds on sperm total motility, at a single concentration of 10^{-8} M, showed that **25** displayed a time-dependent reduction in motility (Figure 5B).

In addition, the compounds inhibited other parameters of sperm motility, including progressive motility, straight line, curvilinear, and average path velocities, linearity, and beat cross frequency (Figure 6A−F). These results show that **10**, **17**, and **25** not only reduce total sperm motility but also directly block all parameters of sperm movement. As observed for total motility, compound **25** was the most effective at decreasing all parameters of sperm motility. We also tested the potential reversibility of effect of compounds **10**, **17** and **25**. For this, we treated rat sperm in the absence and presence of each compound and then measured sperm motility, before and after washing the cells three times with medium. This

procedure did not significantly affect sperm motility in the untreated samples; however, the sperm motility reduction caused by **10**, **17**, and **25** did not recover after the washout, at least for a period of 2 h (Figure 7). Although these experiments do not directly quantify the reversibility of binding of the compounds to their sperm target, they suggest that ouabain analogues have a long-lived effect on sperm motility, at least for the time points used in our study.

We have previously shown that the Na$^+$ and K$^+$ ion gradients created by Na,K-ATPase $\alpha4$ activity are essential to maintain vital parameters of sperm function. Na,K-ATPase $\alpha4$ is required to maintain sperm plasma membrane potential (V_m), intracellular calcium concentration ($[Ca^{2+}]_i$), and cell pH.[32] Accordingly, sperm from mice, in which Na,K-ATPase $\alpha4$ has been knocked out, exhibit depolarization of the plasma membrane, higher $[Ca^{2+}]_i$ levels, and cytoplasm acidification.[19] To test whether ouabain derivatives can alter sperm parameters specifically dependent on Na,K-ATPase $\alpha4$, we determined the effect of our most active compound, **25**, in rat sperm V_m, pH, and $[Ca^{2+}]_i$. Cells were treated in the absence and presence of 10^{-8} M **25** for 1 h, and sperm V_m, pH, and $[Ca^{2+}]_i$ were determined with different fluorophores as described.[19] Compound **25** produced sperm plasma membrane depolarization, increasing V_m by approximately 40% (Figure 8A). Compound **25** also caused intracellular sperm acidification (Figure 8B). Finally, **25** increased $[Ca^{2+}]_i$ in sperm by approximately 40% (Figure 8C). These results agree with the notion that **25** specifically targets Na,K-ATPase $\alpha4$.

Besides being essential determinants of sperm flagellar beat,[57−60] intracellular pH, V_m, and $[Ca^{2+}]_i$, parameters controlled by $\alpha4$ are required for sperm capacitation. An event associated with sperm capacitation is hyperactivation, a
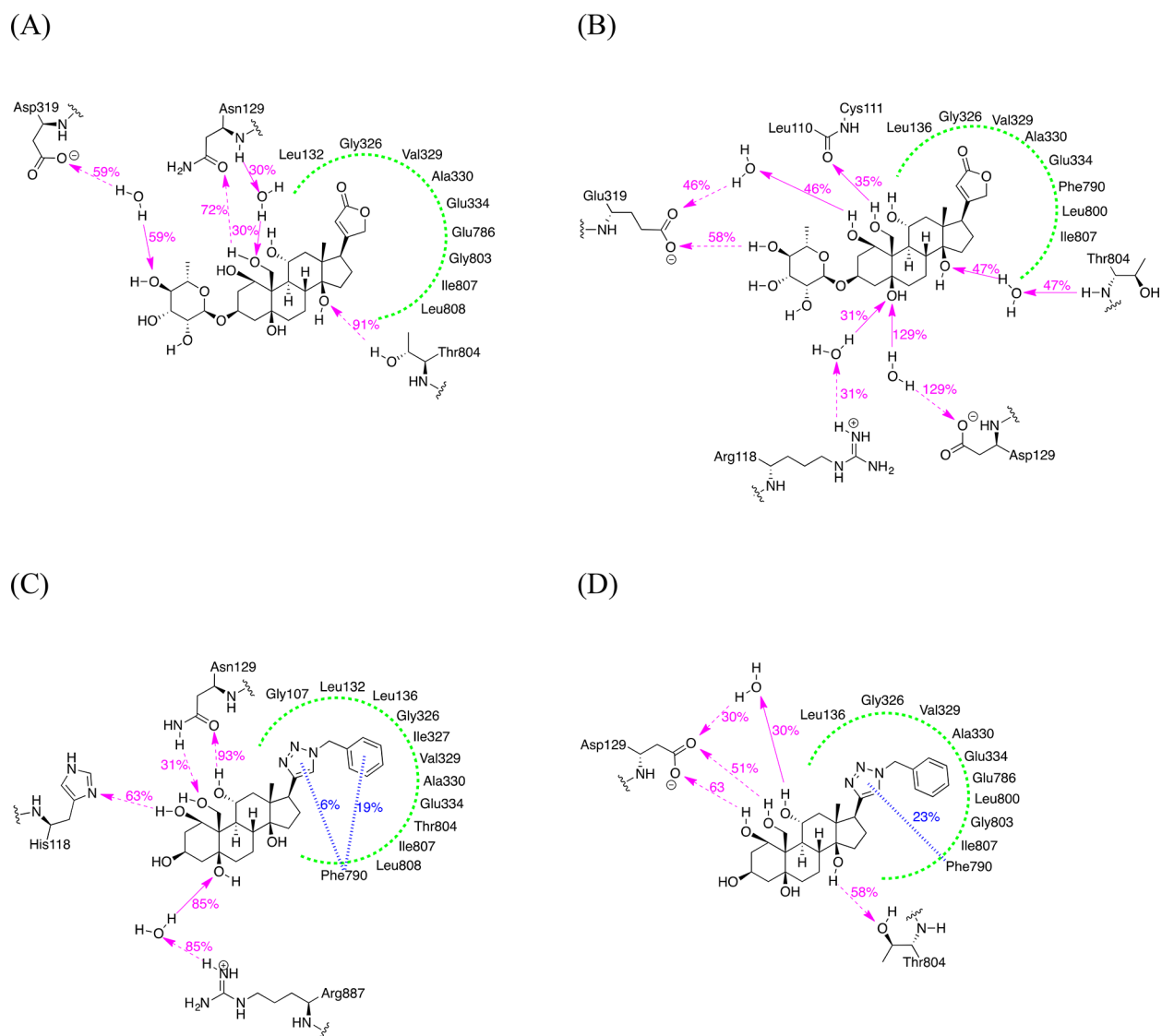
Figure 4. Simulation interaction diagram obtained from the MD simulations of the ligand−protein complexes (from 5 to 18 ns). (A) Ouabain with the rat α4 isoform, (B) ouabain with the rat α1 isoform, (C) compound **25** with the rat α4 isoform, and (D) compound **25** with the rat α1 isoform. The amino acid residue numbers are based on those for the rat α1 in the uniprot database (ID: P06685). The solid magenta arrows represent hydrogen bonding interactions with the backbone of the protein, the dashed magenta arrows hydrogen bonding interactions with the side chains of the protein, green dotted lines hydrophobic surface, and the blue hashed lines π−π interactions.

particular pattern of motility that allows sperm to gain their fertilizing capacity.[61] Compound **25** significantly reduced the hyperactivation accompanying sperm capacitation by approximately 70% (Figure 9). These results show that compound **25** not only reduces sperm motility in general but also specifically interferes with the hyperactivation that sperm acquire when capacitated.

To determine whether ouabain analogues had activity in vivo, we tested the effect of our most potent compound by administering **25** to rats by oral gavage. Prior to in vivo testing, several assays were performed with the compound, including metabolic stability and toxicity assessment. Compound **25** had a high metabolic stability in liver microsomes, which indicated a low metabolic turnover for the compound (Table 3). Permeability, studied in Caco-2 cell monolayers cultured in vitro, showed a very low passage of compound **25** from the apical to the basolateral side of the cells and vice versa. This indicated that the compound has a low permeability across this

epithelium (Table 4). The low in vitro permeability suggests that compound **25** has a low oral absorption consistent with the relatively high oral doses required for in vivo studies using this picomolar Na,K-ATPase inhibitor. Antiproliferation dose−response assays for compounds **10**, **17**, and **25** against MCF-7 breast cancer cells were performed to assess the toxicity of the compounds using ouabain as the positive control. The tested compounds did not exert any antiproliferative activity up to 100 μM (Supporting Information, Figure 2). The effect of ouabain and compounds **10**, **17**, and **25** was evaluated in a competitive displacement fluorescence polarization assay using membranes from cells stably expressing hERG (Invitrogen, Carlsbad, CA). The hERG assay was carried out using E-4031 and fluoxetine as positive controls. Compounds **10**, **17**, and **25** did not inhibit the binding of the fluorescently tagged hERG ligand at concentrations up to 60 μM, whereas ouabain inhibited hERG binding with an IC_{50} of 5.8 μM (Supporting Information, Figure 3). On the basis of these studies, **25**
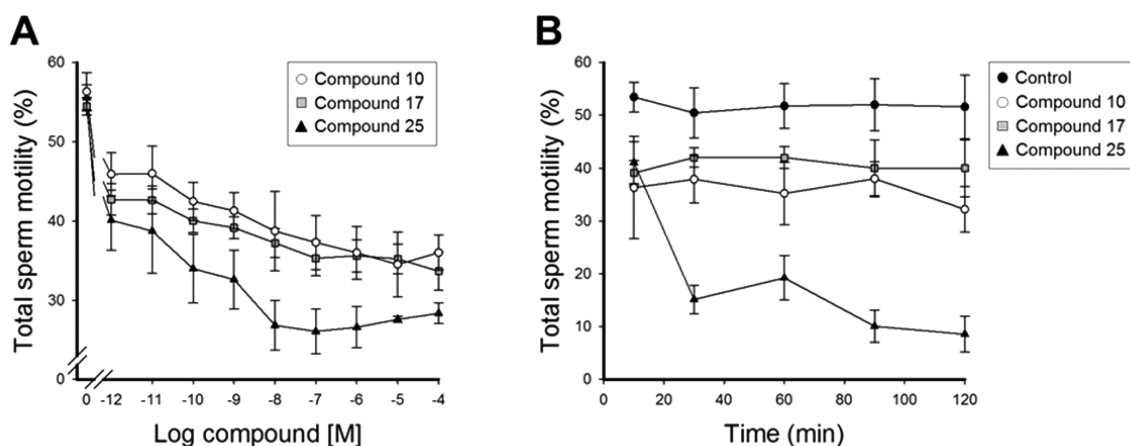
Figure 5. Effect of compounds **10**, **17**, and **25** on rat sperm motility. (A) Dose−response curve for the effect of compounds **10**, **17**, and **25** on total sperm motility after 1 h of incubation. Sperm were collected from the cauda epididymis of rats, and after 1 h incubation, sperm movement was determined by CASA. Values are the mean ± SEM of three determinations. (B) Time dependence for the effect of **10**, **17**, and **25** on total sperm motility. Rat sperm were treated in the absence (control) or presence of 10^{-8} M of the indicated compound. Sperm total motility was assessed as mentioned in part A. Values are the mean ± SEM of three determinations. The data points of compound **25**, after treatment for 30 min and longer were statistically different from those of compounds **10** and **17** and the control, with $P < 0.001$.
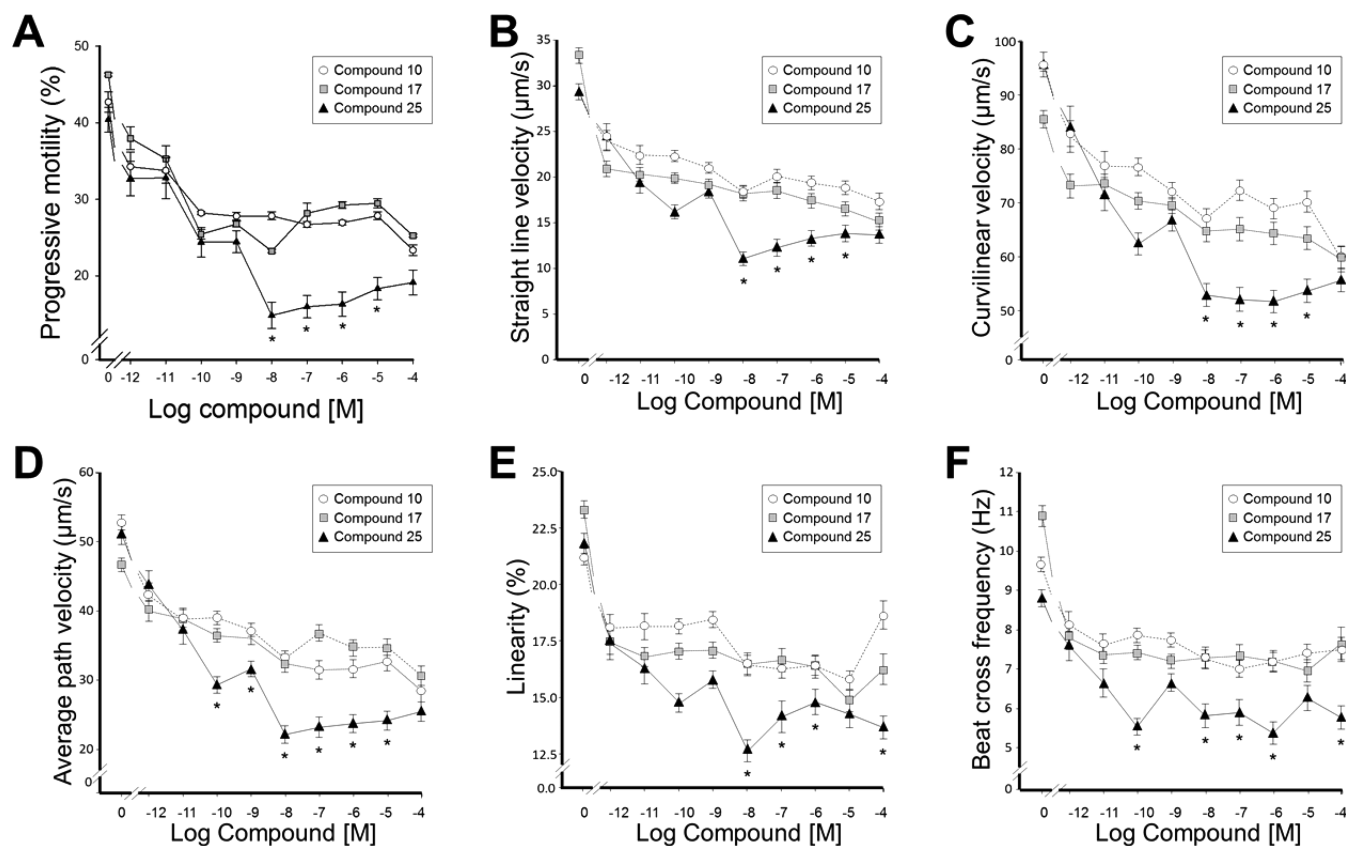

Figure 6. Effect of **10**, **17**, and **25** on different parameters of rat sperm motility. Rat sperm was collected from the cauda epididymis and treated in the absence or presence of the indicated concentrations of each compound. After 1 h of incubation, different patterns of sperm movement were determined by CASA. (A) Progressive motility, (B) straight line velocity, (C) curvilinear velocity, (D) average path velocity, (E) linearity, and (F) beat cross frequency. Values are the mean ± SEM of three determinations. Asterisks indicate statistical differences between compound **25** vs compounds **10** and **17**, with $P < 0.05$.

exhibits a high metabolic stability and a low permeability across epithelia, and it appears not to possess hERG liability.

We next studied the in vivo effects of **25** by administering the compound to rats by oral gavage following two different protocols. In one, male rats were treated orally with three doses of compound **25** (5, 10, and 20 mg/kg) daily for a total of 3 days. In the other, a daily dose of 5 mg/kg weight was given for a duration of 3, 6, 9, or 12 days. After treatment, animals were sacrificed; sperm was collected from the cauda epididymis, and sperm motility was measured by CASA. Compound **25** inhibited sperm total (Figure 10A) and progressive motility (Figure 10B) at the lowest dose used (5 mg/kg) and caused
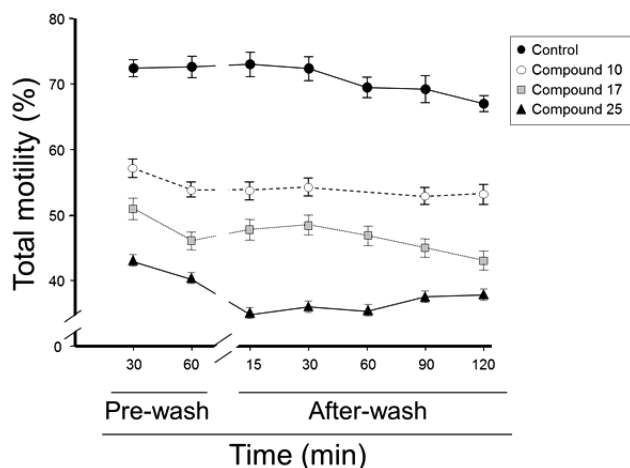
Figure 7. Persistent reduction in sperm motility by compounds **10**, **17**, and **25**. Rat sperm, obtained from the cauda epididymis, was treated in the absence (black circles) and presence of 10^{-8} M of each of the compounds (empty circles, compound **10**; gray squares compound **17**; and black triangles, compound **25**). Sperm motility was measured by CASA, before and after washing the cells three times in Tyrode's modified medium, at the indicated times. Values are the mean ± SEM of three determinations. Comparison of the data points for each compound and the untreated controls as well as among the different compounds showed statistical differences with $P < 0.05$. No statistical differences were found for the values of any of the particular compounds before and after the wash.

approximately a 50% decrease in sperm movement at the highest dose tested (20 mg/kg). A dose of 5 mg/kg produced a maximum of ~40% reduction of total motility and ~50% reduction of progressive motility following 6−12 days of treatment (Figures 10C,D). These results show that compound **25** is able to not only interfere with sperm motility in vitro but also has activity after in vivo administration.

■ DISCUSSION AND CONCLUSIONS

In this work, we have targeted the testis-specific Na,K-ATPase α4 isoform with synthetic cardenolides to pharmacologically interfere with its activity and sperm function. The rationale for selecting Na,K-ATPase α4 as the target is the postmeiotic expression of this protein and the essential role that it plays in sperm motility and capacitation. These characteristics provide
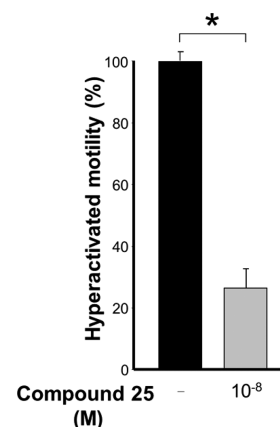

Figure 9. Effect of compound **25** on sperm hyperactivated motility. Sperm from the cauda epididymis were isolated and capacitated in Tyrode's modified medium supplemented with albumin, bicarbonate, and calcium and in the absence (black bar) or presence (gray bar) of 10^{-8} M compound **25** for 1 h. Sperm motility was determined using CASA. Bars represent the mean ± SEM of three experiments. Statistical significance between samples treated with or without compound **25** are indicated with an asterisk, with P values ranging between 0.05 and 0.001.

Table 3. Metabolic Stability of Ouabain Analogue 25[a] in Vitro

	species[b]				
	mouse	rat	dog	monkey	human
percent remaining (%)	76	95	99	89	107

[a]Compound **25** was incubated with liver microsomes, and the remaining levels of compounds were determined after the incubation for 60 min at 37 °C. Reference compound data are shown in the Supporting Information, Table 2. [b]Test concentration was 1×10^{-6} M.

the advantage of blocking sperm function without affecting undifferentiated male germ cells, which allows for a temporary and reversible inhibition of male fertility.[14] In addition, Na,K-ATPase α4 has a uniquely high affinity for the specific inhibitor ouabain relative to the other Na,K-ATPase isoforms.[35] By exploiting this biochemical property, we synthesized ouabain analogues in which the aglycone and lactone ring domains of
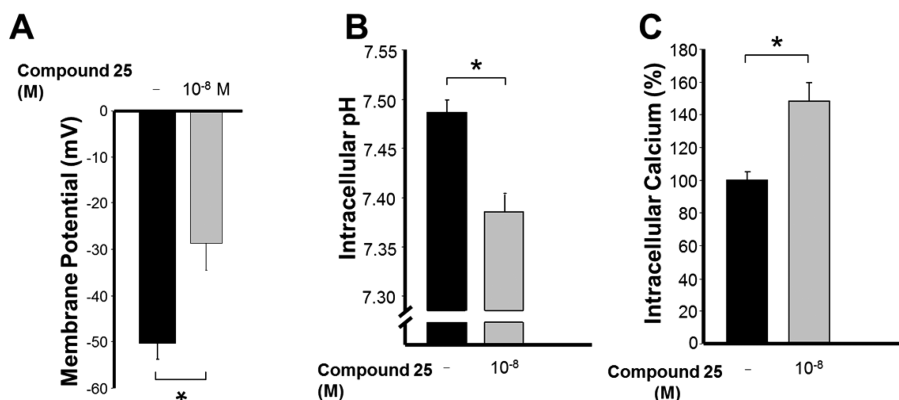
Figure 8. Effect of **25** on different biomarkers of Na,K-ATPase α4 activity. Sperm from the cauda epididymis was isolated in modified Tyrode's medium and treated in the absence and presence of 10^{-8} M **25** for 1 h. Then, (A) sperm V_m was measured using the fluorescent marker DiSC3(5); (B) sperm pH was determined with SNARF-1, and (C) sperm $[Ca^{2+}]_i$ was assessed by calcium green. Bars are the mean ± SEM of three determinations, and asterisks show statistically significant differences, with $P < 0.001$.

Table 4. Permeability of Ouabain Analogue 25 across Epithelia[a]

assay[b]	permeability (10^{-6} cm/s)			flag	percent recovery (%)
	1st	2nd	mean		
A-B permeability (Caco-2, pH 6.5/7.4)	0.19	0.19	<0.2	BLQ	94
B-A permeability (Caco-2, pH 6.5/7.4)	0.14	0.47	0.3		98

[a]Caco-2 cell monolayers cultured to confluence were used to study both apical to basal and basal to apical movements of compound 25. Reference compound data are shown in the Supporting Information, Table 3. The test compound was detected in the donor sample but was not detected in the receiver sample. The concentration of test compound in the receiver sample was below the limit of quantitation (BLQ). [b]Test concentration was 1×10^{-6} M.

the cardenolides were modified. Compounds 10, 17, and 25 showed an improved ability to inhibit Na,K-ATPase α4 compared to ouabain. Thus, dose−response curves for the effect of the compounds on Na,K-ATPase enzymatic activity showed effects at nanomolar and even picomolar concentrations. The ouabain analogues exhibited a higher inhibitory effect on the testis-specific Na,K-ATPase α4 compared to the somatic forms of Na,K-ATPase (α1, α2, α3). Importantly, this selectivity for the Na,K-ATPase α4 isoform specificity is higher for the ouabain analogues than that shown for ouabain.[35] This suggests that 10, 17, and 25 are cardenolides with not only an enhanced activity as blockers of Na,K-ATPase α4 but also an improved selectivity toward close structural isoforms. The SAR studies with the cardenolides and glycosides led to the conclusions that the sugar moiety was not important for the inhibition of the Na,K-ATPase α4 isoform activity (see compounds 10 and 17) and that the C17 substituent is the most important moiety (compare 10 and 17 and 25) for binding. The modifications of the C17 position significantly increased selectivity for the α4 isoform for all three inhibitors shown in Table 2. Compound 25, carrying a benzyltriazole moiety at C17, is a subnanomolar inhibitor of the α4 isoform with an outstanding α4 isoform selectivity profile. The results also indicate that the free hydroxyl groups located on the northern part of the molecule are not essential for potency and selectivity (compare 10 and 17 and 25). Of interest is the finding that a C17 hydroxymethyl group and a C17 benzyltriazole group both confer a high α4 selectivity.

Homology models of the rat isoforms were prepared in order to understand the structural origin of the selectivity of these compounds toward the rat α4 over the rat α1 isoform. MD simulations of the complexes of the rat α4 with ouabain and 25 provided information about the potential interactions between the pocket and the ligand such as hydrogen bonding and electrostatic, π−π, and hydrophobic interactions. Strong hydrogen bonding interactions between rat Na,K-ATPase α4 residues Asn129 and His118 with 1-OH, 11-OH, and 19-OH are postulated to confer α4 selectivity for compound 25. Water-mediated hydrogen bonding interaction of Arg887 of the α4 with 5-OH of compound 25 further enhances the binding interactions

Consistent with their activity as inhibitors of Na,K-ATPase α4, compounds 10, 17, and 25 were able to interfere with sperm motility. The compounds not only affected total sperm motility but also affected a variety of sperm motility patterns, including progressive motility, straight line, curvilinear, average path velocities, linearity, and beat cross frequency. This overall effect on sperm movement agrees with our previous results, showing that the Na,K-ATPase α4 function is essential for supporting all aspects of sperm movement.[19] Compounds 10, 17, and 25 do not completely block motility as these compounds cause a maximum of ∼50−60% reduction of sperm motility even at high concentrations. According to the World Health organization (WHO), the lower reference limits for normal sperm motility are approximately 40% sperm motility, and 50% or less is a predictor of male infertility.[62] Therefore, the capacity of ouabain analogues to reduce sperm motility already approaches what is required to produce male infertility. While compounds 10, 17, and 25 do not completely inhibit sperm motility, they provide a valuable chemical scaffold for further development of a male contraceptive agent. Interestingly, compound 25 produced even a higher reduction of hyperactivated motility, decreasing this type of sperm movement by approximately 70%. Hyperactivation is one of the main events that accompany sperm capacitation, and it is essential for the ability of sperm to fertilize the egg.[63−65] Therefore, 25 has a dual effect, not only decreasing the ability of sperm to swim and reach the egg but also reducing the hyperactivated pattern of sperm motility to a greater extent, which is necessary for sperm to penetrate the egg zona pellucida. This dual effect of 25, on overall motility and particularly hyperactivation, makes it a desirable candidate for male contraception.
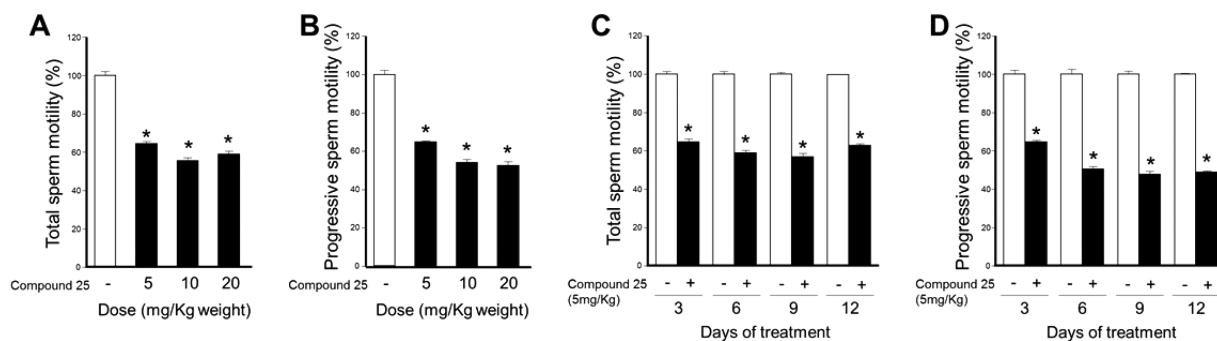
Figure 10. Effect of compound 25 on rat total and progressive sperm motility in vivo. Compound 25 was administered by oral gavage at different doses (5, 10, and 20 mg/kg of body weight) for 3 days (A, B) or at 5 mg/kg of body weight for the indicated times (C, D). Total and progressive sperm motility was determined on sperm from the cauda epididymis using CASA. Bars represent the mean ± SEM of three experiments. Values significantly different from the untreated controls are indicated with an asterisk, with $P \geq 0.05$.

Our results show that the effect of compounds **10**, **17**, and **25** were not rapidly reversible, at least for the time period in which sperm motility could be confidently tested. The effect at longer times could not be assessed because of the natural decrease in sperm movement that occurs during sperm manipulation in vitro, an effect that is especially marked for rat sperm.[66] It has been shown that the long duration of the effect of ouabain on Na,K-ATPase is due to the low dissociation rate from the enzyme.[67−69] The higher inhibitory potency of ouabain for the Na,K-ATPase α2 and α3 isoforms compared to α1 depends on the lower dissociation rate of ouabain for α2 and α3.[70] While additional experiments will be needed to calculate the kinetics of ouabain analogues binding to Na,K-ATPase α4, it is likely that these very high affinity inhibitors have very slow dissociation rates from the enzyme. Additional support for this hypothesis is our observation that, following systemic in vivo dosing with compound **25**, the Na,K-ATPase remains inhibited during the time required to remove sperm and determine motility. The low reversibility of ouabain analogues, common to other cardenolides, represents an advantage for the potential use of these compounds as male contraceptives, for which a prolonged effect is desired.

We found that compound **25** depolarizes sperm membrane potential, which agrees with the idea that inhibition of Na,K-ATPase α4 ion transport results in a dissipation of the ion gradient that exists between the sperm cytosol and the environment.[32] Also, compound **25** causes acidification of the sperm cytoplasm and an increase in $[Ca^{2+}]_i$. These effects are similar to those previously observed when sperm is subjected to relatively low doses of ouabain, which preferentially inhibits Na,K-ATPase α4. Therefore, similar to ouabain, compound **25** likely increases intracellular Na^+ concentrations in sperm, which decreases the Na^+ gradient across the sperm plasma membrane and the driving force for H^+ and Ca^{2+} extrusion out of the cells.[32] This mechanism of action is in good agreement with the effects observed when Na,K-ATPase α4 is knocked out in mice.[19] Therefore, cell membrane depolarization, cytosol acidification, and rise in $[Ca^{2+}]_i$, all parameters that depend on Na,K-ATPase α4 activity, are affected by compound **25**. The tight regulation of V_m, pH, and $[Ca^{2+}]_i$ is essential for sperm motility and capacitation. Therefore, the effects that compound **25** causes on these parameters most likely reflects its inhibition of Na,K-ATPase α4, resulting in a decreased sperm function.

Importantly, compound **25** not only reduces sperm motility in vitro but also reduces sperm motility in vivo. Thus, after administration to rats, compound **25** decreased sperm motility as soon as 3 days after administration and with doses as low as 5 mg/kg. This suggests that the compound is reaching its target cells and that its effects persist even after sperm is isolated from the rat epididymis. Importantly, compound **25** did not exert any major toxic effect on treated rats. This agrees with our results from general preliminary in vitro toxicity assays, such as the antiproliferative and hERG assays. It is important to note that compounds **10**, **17**, and **25** had little effect on proliferation of MCF-7 cells. The reduced effect of the compounds on a human cell line supports the Na,K-ATPase isoform selectivity of action of the compounds and suggests that they could have a safe use in humans. In addition, the reduced effect of compound **25** in the hERG assays highlights the improved safety margin that the compounds have compared to ouabain and other cardiotonic steroids. Regarding accessibility of compound **25** to sperm following systemic dosing, it is apparent that compound **25** is able to reach spermatozoa,

either at the level of the testis or later in the male reproductive tract. The blood−testis barrier is known to tightly restrict the passage of molecules to the seminiferous tubule lumen.[71] The steroidal nature of compound **25** may allow it to cross the Sertoli cell tight junctions to reach the sperm. Alternatively, compound **25** may have a better chance to affect the sperm in the epididymis, where the epithelium of the tubules is relatively more permeable than the testis seminiferous tubules,[72,73] or in the ejaculate, through its secretion via the different accessory glands present along the male reproductive tract. Additional experiments will be required to determine the distribution of ouabain analogues to different regions of the male reproductive tract; however, at the present time, our study establishes important proof of principle for the potential use of these types of compounds as effective blockers of sperm function.

In conclusion, we have synthesized new cardenolides with improved selectivity for inhibition of the Na,K-ATPase α4 isoform, which interfere with sperm motility and sperm hyperactivation. This novel scaffold represents an attractive chemical structure for further development of a highly specific male contraceptive.

■ EXPERIMENTAL SECTION

Chemistry General. All chemicals and reagents were purchased from commercial sources and used directly without further purification. Solvents were dried using standard procedures. All nonaqueous reactions were performed under an atmosphere of nitrogen in oven-dried glassware. Reaction progress was monitored by thin-layer chromatography using silica gel plates (silica gel 60 F254), and eluted TLC plates were visualized with UV light (254 nm) or developing the plate with $Ce(SO_4)_2$ stain. The products were isolated and purified by flash column chromatography. NMR experiments were performed on a 400/100 MHz instrument. NMR spectra were processed with the MestReNova program. Chemical shifts were reported as ppm relative to $CDCl_3$ (7.26 ppm for ^{1}H, 77.0 ppm for ^{13}C), CD_3OD (3.31 and 4.87 ppm for ^{1}H, 49.1 ppm for ^{13}C), and DMSO-d_6 (2.50 ppm for ^{1}H, 39.5 ppm for ^{13}C). ^{1}H NMR coupling constants (J) are expressed in hertz (Hz), and multiplicity is described as follows: s = singlet; d = doublet; t = triplet; q = quartet; p = pentet; br = broad; m = multiplet. High-resolution mass spectra and electrospray (ESI) experiments were recorded with electron-spray ionization. Melting points were determined with a melting point apparatus and were uncorrected. All of the tested compounds were determined to be pure (≥95%) by LC-MS except for compounds **11** (≥90%), **19** (≥85%), and **30** (≥85%).

4-((3R,3aR,5R,5aS,5bR,9aR,11S,12aS,14aR,14bS)-5,12a,14b-Tri-hydroxy-11-(((3aR,4R,6S,7S,7aR)-7-hydroxy-2,2,6-trimethyltetrahy-dro-4H-[1,3]dioxolo[4,5-c]pyran-4-yl)oxy)-3a,8,8-trimethylhexade-cahydro-6H-cyclopenta[7,8]phenanthro[4,4a-d][1,3]dioxin-3-yl)-furan-2(5H)-one (1). To a stirred suspension of ouabain octahydrate (2.50 g, 3.42 mmol) in acetone (100 mL) was added concentrated hydrochloric acid (0.100 mL) at room temperature. After the mixture was stirred for 2 h, the reaction mixture was neutralized with Et_3N (1.00 mL); volatiles were evaporated, and then water (50 mL) was added. The mixture was extracted with CH_2Cl_2 (3 × 50 mL), which was then dried over Na_2SO_4 and concentrated under reduced pressure. The residue was purified by column chromatography (silica gel, CH_2Cl_2/EtOH, 9:1) to provide **1** (1.91 g, 84%) as a white solid: mp 182−184 °C; $[\alpha]_D^{22}$ +2.48 (c 0.442, $CHCl_3$); ^{1}H NMR (400 MHz, $CDCl_3$) δ 5.91 (s, 1H), 5.15 (s, 1H), 5.03 (s, 1H), 4.87 (ddd, J = 51.7, 18.1, 1.6 Hz, 2H), 4.60−4.44 (m, 2H), 4.27−4.11 (m, 4H), 4.01 (p, J = 6.3 Hz, 1H), 3.73 (d, J = 12.3 Hz, 1H), 3.51 (dd, J = 12.6, 6.6 Hz, 1H), 2.97−2.86 (m, 1H), 2.82 (d, J = 7.0 Hz, 1H), 2.24−1.65 (m, 10H), 1.63−1.48 (m, 8H), 1.46−1.26 (m, 14H), 1.20−1.07 (m, 1H), 0.95 (s, 3H); ^{13}C NMR (100 MHz, $CDCl_3$) δ 174.1, 172.8, 118.1, 109.4, 101.3, 96.8, 84.1, 74.9, 73.3, 72.9, 72.7, 72.4, 68.5, 68.0, 67.3, 60.4, 50.0, 49.2, 49.0, 47.4, 46.2, 41.0, 36.0, 34.7, 33.6, 30.4, 29.6, 27.3,

26.7, 25.6, 24.6, 23.0, 22.7, 18.7, 17.2; HRMS (ESI) calcd for $C_{35}H_{53}O_{12}$ [M + H]$^+$ 665.3537, found 665.3532.

4-((3R,3aR,5R,5aS,5bR,9aR,11S,12aS,14aR,14bS)-12a,14b-Dihydroxy-5-(methoxymethyl)-11-(((3aR,4R,6S,7S,7aR)-7-(methoxymethyl)-2,2,6-trimethyltetrahydro-4H-[1,3]dioxolo[4,5-c]pyran-4-yl)oxy)-3a,8,8-trimethylhexadecahydro-6H-cyclopenta[7,8]phenanthro[4,4a-d][1,3]dioxin-3-yl)furan-2(5H)-one (2). To a solution of **1** (2.70 g, 4.06 mmol) and diisopropylethylamine (5.67 mL, 32.5 mmol) in CH$_2$Cl$_2$ (75 mL) was added chloromethyl methyl ether (MOM-Cl) (1.22 mL, 16.3 mmol) at 0 °C. The reaction mixture was stirred at room temperature for 12 h and then diluted with water (75 mL). The organic phase was separated, and the aqueous layer was extracted with additional CH$_2$Cl$_2$ (3 × 50 mL). The combined extracts were washed with brine (50 mL) and dried over Na$_2$SO$_4$. Volatiles were removed under reduced pressure, and the crude product was purified by column chromatography (silica gel, hexanes/ethyl acetate, 3:7) to yield compound **2** (2.07 g, 68%) as a yellow foam: ^{1}H NMR (400 MHz, CDCl$_3$) δ 5.89 (s, 1H), 5.11 (s, 1H), 4.96 (d, J = 6.4 Hz, 1H), 4.91–4.76 (m, 2H), 4.72 (q, J = 6.5 Hz, 3H), 4.66 (d, J = 6.4 Hz, 1H), 4.58 (s, 1H), 4.46 (d, J = 12.3 Hz, 1H), 4.13 (dd, J = 13.6, 8.0 Hz, 2H), 4.07 (d, J = 5.5 Hz, 1H), 4.04–3.90 (m, 2H), 3.62 (t, J = 15.5 Hz, 1H), 3.40 (dd, J = 15.5, 8.7 Hz, 7H), 3.00 (t, J = 7.6 Hz, 1H), 2.17–1.45 (m, 16H), 1.42–1.19 (m, 15H), 1.11 (m, 1H), 0.88 (s, 3H); ^{13}C NMR (100 MHz, CDCl$_3$) δ 174.0, 172.4, 117.7, 109.1, 100.9, 97.0, 96.8, 96.3, 83.6, 78.3, 78.1, 76.5, 75.8, 73.3, 72.96, 72.91, 66.6, 64.7, 60.5, 56.1, 55.8, 49.5, 48.3, 47.5, 45.3, 44.1, 40.8, 35.8, 34.5, 33.9, 30.4, 27.9, 26.6, 26.5, 24.8, 23.0, 22.7, 17.7, 17.5; HRMS (ESI) calcd for $C_{39}H_{61}O_{14}$ [M + H]$^+$ 753.4061, found 753.4054.

(3S,3aR,5R,5aS,5bR,9aR,11S,12aS,14aR,14bS)-3-((R)-1,2-Dihydroxyethyl)-5-(methoxymethyl)-11-(((3aR,4R,6S,7S,7aR)-7-(methoxymethyl)-2,2,6-trimethyltetrahydro-4H-[1,3]dioxolo[4,5-c]pyran-4-yl)oxy)-3a,8,8-trimethyltetradecahydro-6H-cyclopenta[7,8]phenanthro[4,4a-d][1,3]dioxine-12a,14b-diol and (3S,3aR,5R,5aS,5bR,9aR,11S,12aS,14aR,14bS)-3-((S)-1,2-Dihydroxyethyl)-5-(methoxymethyl)-11-(((3aR,4R,6S,7S,7aR)-7-(methoxymethyl)-2,2,6-trimethyltetrahydro-4H-[1,3]dioxolo[4,5-c]pyran-4-yl)oxy)-3a,8,8-trimethyltetradecahydro-6H-cyclopenta[7,8]phenanthro[4,4a-d][1,3]dioxine-12a,14b-diol (3). Ozone was bubbled through a solution of **2** (2.50 g, 3.32 mmol) in CH$_2$Cl$_2$ (60 mL) at −78 °C for 1 h, and then the mixture was stirred at −78 °C for 2 h. The solution was degassed with nitrogen, and then Zn (11.9 g, 182 mmol) and AcOH (12.4 mL, 216 mmol) were added; the mixture was stirred for an additional 2 h at room temperature. The solution was filtered, and then the volatiles were removed under reduced pressure to obtain the corresponding ester (2.20 g), which was used for the next step without further purification.

To a solution of the above ester (2.20 g) in methanol (30 mL) was added KHCO$_3$ (0.830 g, 8.38 mmol) in water (5 mL). After the mixture was stirred for 3 h at room temperature, the volatiles were removed and then water (50 mL) was added to the residue, which was then extracted with ethyl acetate (3 × 50 mL). The combined organic layers were dried over Na$_2$SO$_4$ and filtered, and the solvent was removed under reduced pressure to provide the unstable hydroxymethyl ketone (1.25 g), which was immediately subjected to the next step.

The above crude hydroxymethyl ketone (1.25 g) was dissolved in methanol (30 mL) and cooled to 0 °C. Sodium borohydride (0.460 g, 12.4 mmol) was added to the reaction mixture, and the reaction mixture was stirred for 30 min. Then saturated aqueous NH$_4$Cl (30 mL) was added, after which the reaction mixture was extracted with ethyl acetate (3 × 30 mL). The organic layers were combined, dried over Na$_2$SO$_4$, and filtered. The solvent was removed under reduced pressure, and the resultant residue was purified by column chromatography (silica gel, hexanes/ethyl acetate, 1:9) to afford a diastereomeric mixture (3:2) of diol **3** (1.01 g, 42% for three steps) as a white solid: mp 119–121 °C; [α]$_D^{22}$ −16 (c 0.71, CHCl$_3$); ^{1}H NMR (400 MHz, CDCl$_3$) δ 5.11 (s, 1H), 4.96 (d, J = 6.4 Hz, 1H), 4.91 (s, 0.5H), 4.82 (d, J = 6.5 Hz, 0.5H), 4.76–4.63 (m, 3H), 4.52–4.40 (m, 2H), 4.19–4.02 (m, 3H), 4.01–3.59 (m, 5H), 3.47–3.34 (m, 8H), 2.24–1.17 (m, 35H), 1.09 (s, 1.6H), 1.08 (s, 1.4H); ^{13}C NMR (100 MHz, CDCl$_3$) δ 109.19, 109.16, 100.88, 100.84, 97.6, 96.87, 96.84,

96.7, 96.3, 83.3, 82.2, 78.3, 78.2, 78.1, 76.1, 74.8, 73.2, 73.1, 73.07, 73.02, 69.9, 67.0, 66.7, 66.4, 65.8, 64.68, 64.63, 60.7, 60.6, 55.9, 55.8, 50.6, 50.0, 47.8, 47.6, 47.1, 47.0, 46.5, 45.3, 44.8, 42.9, 40.3, 39.8, 36.3, 35.6, 34.9, 34.6, 34.1, 32.9, 30.4, 30.2, 27.9, 26.5, 25.2, 24.8, 23.2, 23.1, 22.5, 18.5, 18.1, 17.5, 15.7; HRMS (ESI) calcd for $C_{37}H_{63}O_{14}$ [M + H]$^+$ 731.4218, found 731.4238.

(3S,3aR,5R,5aS,5bR,9aR,11S,12aS,14aR,14bS)-12a,14b-Dihydroxy-5-(methoxymethyl)-11-(((3aR,4R,6S,7S,7aR)-7-(methoxymethyl)-2,2,6-trimethyltetrahydro-4H-[1,3]dioxolo[4,5-c]pyran-4-yl)oxy)-3a,8,8-trimethylhexadecahydro-6H-cyclopenta[7,8]phenanthro[4,4a-d][1,3]dioxine-3-carbaldehyde (4). To a stirred solution of diol **3** (2.50 g, 3.42 mmol) in THF/H$_2$O (8:2, 20 mL) was added sodium periodate (2.18 g, 10.3 mmol). After stirring for 1 h, the reaction was diluted with EtOAc (50 mL). Insoluble materials were filtered off, and the filtrate was washed sequentially with water (30 mL) and brine (30 mL) and dried over Na$_2$SO$_4$. The solvent was then removed under reduced pressure, and the residue was purified by column chromatography (silica gel, hexanes/ethyl acetate, 3:7) to afford aldehyde **4** (1.50 g, 63%) as a foam: ^{1}H NMR (400 MHz, CDCl$_3$) δ 9.72 (s, 1H), 5.12 (s, 1H), 4.98 (d, J = 6.4 Hz, 1H), 4.91–4.79 (m, 2H), 4.71–4.63 (m, 3H), 4.46 (d, J = 12.3 Hz, 1H), 4.20–4.10 (m, 2H), 4.08 (d, J = 5.5 Hz, 1H), 4.02–3.83 (m, 2H), 3.72 (d, J = 12.3 Hz, 1H), 3.49–3.30 (m, 7H), 2.46 (dt, J = 9.0, 3.2 Hz, 1H), 2.28–1.76 (m, 9H), 1.74–1.22 (m, 23H), 1.11 (s, 3H); ^{13}C NMR (100 MHz, CDCl$_3$) δ 205.8, 109.1, 100.9, 97.5, 96.7, 96.3, 83.1, 78.3, 78.2, 76.5, 75.8, 73.1, 72.9, 66.8, 64.6, 61.1, 60.5, 56.0, 55.8, 49.9, 47.8, 45.6, 44.9, 40.0, 36.2, 34.8, 33.2, 30.2, 27.9, 26.5, 24.8, 23.10, 23.06, 20.0, 17.5, 15.9; HRMS (ESI) calcd for $C_{36}H_{59}O_{13}$ [M + H]$^+$ 699.3956, found 699.3977.

(3S,3aR,5R,5aS,5bR,9aR,11S,12aS,14aR,14bS)-3-((R)-1-Hydroxyprop-2-yn-1-yl)-5-(methoxymethyl)-11-(((3aR,4R,6S,7S,7aR)-7-(methoxymethyl)-2,2,6-trimethyltetrahydro-4H-[1,3]dioxolo[4,5-c]pyran-4-yl)oxy)-3a,8,8-trimethyltetradecahydro-6H-cyclopenta[7,8]phenanthro[4,4a-d][1,3]dioxine-12a,14b-diol and (3S,3aR,5R,5aS,5bR,9aR,11S,12aS,14aR,14bS)-3-((S)-1-Hydroxyprop-2-yn-1-yl)-5-(methoxymethyl)-11-(((3aR,4R,6S,7S,7aR)-7-(methoxymethyl)-2,2,6-trimethyltetrahydro-4H-[1,3]dioxolo[4,5-c]pyran-4-yl)oxy)-3a,8,8-trimethyltetradecahydro-6H-cyclopenta[7,8]phenanthro[4,4a-d][1,3]dioxine-12a,14b-diol (5). To a solution of aldehyde **4** (1.00 g, 1.43 mmol) in THF (30 mL) at −78 °C was added an ethynylmagnesium bromide solution (0.5 M in THF, 14.7 mL, 7.15 mmol). After stirring for 1 h, the reaction mixture was quenched with saturated aqueous NH$_4$Cl (30 mL). The organic phase was separated, and the mixture was extracted with EtOAc (2 × 30 mL). The organic layers were dried over Na$_2$SO$_4$ and concentrated under reduced pressure. The residue was purified by column chromatography (silica gel, hexanes/ethyl acetate, 6:4) to yield a diastereomeric mixture (3:1) of alkynol **5** (0.760 g, 74%) as a white foam: ^{1}H NMR (400 MHz, CDCl$_3$) δ 5.10 (s, 1H), 4.96 (d, J = 6.4 Hz, 1H), 4.91 (s, 1H), 4.83 (d, J = 6.5 Hz, 1H), 4.66 (dd, J = 6.3, 3.5 Hz, 3H), 4.54 (s, 1H), 4.44 (d, J = 12.3 Hz, 1H), 4.11 (dd, J = 13.5, 6.3 Hz, 2H), 4.07 (d, J = 5.5 Hz, 1H), 3.94 (dd, J = 9.9, 6.2 Hz, 1H), 3.85–3.57 (m, 2H), 3.47–3.23 (m, 7H), 2.40 (d, J = 2.0 Hz, 1H), 1.96 (ddt, J = 54.1, 42.0, 14.7 Hz, 10H), 1.69–1.19 (m, 24H), 1.09 (s, 0.8H), 1.69 (s, 2.2H).

(3S,3aR,5R,5aS,5bR,9aR,11S,12aS,14aR,14bS)-3-((R)-(1-(4-Fluorobenzyl)-1H-1,2,3-triazol-4-yl)(hydroxy)methyl)-5-(methoxymethyl)-11-(((3aR,4R,6S,7S,7aR)-7-(methoxymethyl)-2,2,6-trimethyltetrahydro-4H-[1,3]dioxolo[4,5-c]pyran-4-yl)oxy)-3a,8,8-trimethyltetradecahydro-6H-cyclopenta[7,8]phenanthro[4,4a-d][1,3]dioxine-12a,14b-diol and (3S,3aR,5R,5aS,5bR,9aR,11S,12aS,14aR,14bS)-3-((S)-(1-(4-Fluorobenzyl)-1H-1,2,3-triazol-4-yl)(hydroxy)methyl)-5-(methoxymethyl)-11-(((3aR,4R,6S,7S,7aR)-7-(methoxymethyl)-2,2,6-trimethyltetrahydro-4H-[1,3]dioxolo[4,5-c]pyran-4-yl)oxy)-3a,8,8-trimethyltetradecahydro-6H-cyclopenta[7,8]phenanthro[4,4a-d][1,3]dioxine-12a,14b-diol (6). To a solution of the 4-fluorobenzyl azide (0.014 g, 0.096 mmol) and alkynol **5** (0.070 g, 0.096 mmol) in DMF (2 mL) was added sodium ascorbate (0.0077 g, 0.038 mmol) in water (1 mL). The reaction mixture was stirred for 2 min, and then CuSO$_4$·5H$_2$O (0.0047 g, 0.0019 mmol) in water (1 mL) was added. The mixture was stirred at room temperature for 12 h; then water (4 mL) was added, and then the mixture was extracted with ethyl acetate (3 ×

5 mL). The combined organic extracts were dried over Na_2SO_4 and evaporated under reduced pressure to afford a green solid, which was purified by column chromatography (silica gel, hexanes/ethyl acetate, 2:8) to give compound **6** (0.035 g, 42%) as a white foam: $[\alpha]_D^{22}$ −15.6 (c 0.379, CHCl₃); ¹H NMR (400 MHz, CDCl₃) δ 7.37 (s, 1H), 7.23 (dd, J = 5.9, 2.7 Hz, 2H), 7.09−7.01 (m, 2H), 5.50−5.41 (m, 2H), 5.08 (d, J = 9.6 Hz, 2H), 4.96 (d, J = 6.5 Hz, 1H), 4.91 (s, 1H), 4.82 (d, J = 6.5 Hz, 1H), 4.69−4.61 (m, 3H), 4.44 (d, J = 12.2 Hz, 1H), 4.16−4.08 (m, 2H), 4.06 (d, J = 5.5 Hz, 1H), 3.94 (dq, J = 12.5, 6.2 Hz, 1H), 3.83 (td, J = 10.9, 5.1 Hz, 1H), 3.78−3.66 (m, 1H), 3.44−3.35 (m, 4H), 3.34 (s, 3H), 2.37−2.26 (m, 1H), 2.14−1.66 (m, 8H), 1.67−1.42 (m, 9H), 1.41−1.15 (m, 18H), 1.08 (dd, J = 23.7, 11.8 Hz, 1H); ¹³C NMR (100 MHz, CDCl₃) δ 161.6, 130.5, 129.9, 129.8, 120.8, 116.2, 116.0, 109.1, 100.8, 97.7, 96.7, 96.3, 83.3, 78.3, 78.2, 76.5, 73.1, 72.9, 66.9, 66.1, 64.3, 60.5, 56.0, 55.8, 54.8, 53.4, 47.8, 47.6, 46.7, 45.4, 40.2, 36.2, 34.9, 32.5, 30.2, 27.9, 26.5, 24.8, 23.1, 18.5, 18.4, 17.5, 15.6; HRMS (ESI) calcd for $C_{45}H_{67}N_3O_{13}F$ [M + H]⁺ 876.4658, found 876.4686.

(3S,3aR,5R,5aS,5bR,9aR,11S,12aS,14aR,14bS)-3-((R)-(1-Benzyl-1H-1,2,3-triazol-4-yl)(hydroxy)methyl)-5-(methoxymethoxy)-11-(((3aR,4R,6S,7S,7aR)-7-(methoxymethoxy)-2,2,6-trimethyltetrahydro-4H-[1,3]dioxolo[4,5-c]pyran-4-yl)oxy)-3a,8,8-trimethyltetradecahydro-6H-cyclopenta[7,8]phenanthro[4,4a-d][1,3]dioxine-12a,14b-diol and (3S,3aR,5R,5aS,5bR,9aR,11S,12aS,14aR,14bS)-3-((S)-1-Benzyl-1H-1,2,3-triazol-4-yl)(hydroxy)methyl)-5-(methoxymethoxy)-11-(((3aR,4R,6S,7S,7aR)-7-(methoxymethoxy)-2,2,6-trimethyltetrahydro-4H-[1,3]dioxolo[4,5-c]pyran-4-yl)oxy)-3a,8,8-trimethyltetradecahydro-6H-cyclopenta[7,8]phenanthro[4,4a-d][1,3]-dioxine-12a,14b-diol (7). Following the procedure described for compound **6**, compound **7** (0.075 g, 64%) was obtained as a white foam and used without further characterization for the synthesis of compound **9**.

(1R,3S,5S,8R,9S,10R,11R,13R,14S,17S)-17-((R)-(1-(4-Fluorobenzyl)-1H-1,2,3-triazol-4-yl)(hydroxy)methyl)-10-(hydroxymethyl)-13-methyl-3-(((2R,3R,4R,5R,6S)-3,4,5-trihydroxy-6-methyltetrahydro-2H-pyran-2-yl)oxy)tetradecahydro-5H-cyclopenta[a]-phenanthrene-1,5,11,14(2H)-tetraol and (1R,3S,5S,8R,9S,10R,11R,13R,14S,17S)-17-((S)-(1-(4-Fluorobenzyl)-1H-1,2,3-triazol-4-yl)(hydroxy)methyl)-10-(hydroxymethyl)-13-methyl-3-(((2R,3R,4R,5R,6S)-3,4,5-trihydroxy-6-methyltetrahydro-2H-pyran-2-yl)oxy)tetradecahydro-5H-cyclopenta[a]-phenanthrene-1,5,11,14(2H)-tetraol (8). Compound **6** (0.035 mg, 0.040 mmol) was dissolved in 4 N HCl in MeOH (5 mL), and the solution was stirred at room temperature for 12 h. After completion of the reaction (monitored by TLC), the solvent was removed under reduced pressure. The residue was purified by flash column chromatography (silica gel, EtOAc/MeOH, 8:2 with 2% water) to furnish compound **8** (0.012 g, 42%) as a white foam: $[\alpha]_D^{22}$ −81.1 (c 0.148, MeOH); ¹H NMR (400 MHz, CD₃OD) δ 7.95 (s, 1H), 7.39 (dd, J = 8.6, 5.3 Hz, 2H), 7.22−6.97 (m, 2H), 5.61 (d, J = 8.4 Hz, 2H), 5.01 (s, 1H), 4.25 (m, 4H), 3.83−3.61 (m, 3H), 3.45−3.27 (m, 3H), 2.30−1.88 (m, 6H), 1.87−1.16 (m, 17H); HRMS (ESI) calcd for $C_{35}H_{50}FN_3O_{11}$ [M + Na]⁺ 730.3327, found 730.3328.

(1R,3S,5S,8R,9S,10R,11R,13R,14S,17S)-17-((R)-(1-Benzyl-1H-1,2,3-triazol-4-yl)(hydroxy)methyl)-10-(hydroxymethyl)-13-methyl-3-(((2R,3R,4R,5R,6S)-3,4,5-trihydroxy-6-methyltetrahydro-2H-pyran-2-yl)oxy)tetradecahydro-5H-cyclopenta[a]phenanthrene-1,5,11,14(2H)-tetraol and (1R,3S,5S,8R,9S,10R,11R,13R,14S,17S)-17-((S)-(1-Benzyl-1H-1,2,3-triazol-4-yl)(hydroxy)methyl)-10-(hydroxymethyl)-13-methyl-3-(((2R,3R,4R,5R,6S)-3,4,5-trihydroxy-6-methyltetrahydro-2H-pyran-2-yl)oxy)tetradecahydro-5H-cyclopenta[a]phenanthrene-1,5,11,14(2H)-tetraol (9). This compound was obtained from intermediate **7**, following the procedure described for compound **8**. Compound **9** was obtained (0.016 g, 40%) as a white foam: $[\alpha]_D^{22}$ −42.5 (c 0.214, MeOH); ¹H NMR (400 MHz, CD₃OD) δ 8.06 (s, 1H), 7.38 (t, J = 9.5 Hz, 5H), 5.66 (d, J = 10.3 Hz, 2H), 5.03 (d, J = 44.3 Hz, 1H), 4.25 (m, 4H), 3.84−3.62 (m, 3H), 3.41−3.33 (m, 3H), 2.28−1.86 (m, 6H), 1.85−1.17 (m, 17H); HRMS (ESI) calcd for $C_{35}H_{51}N_3O_{11}Na$ [M + Na]⁺ 712.3421, found 712.3425.

(3S,3aR,5R,5aS,5bR,9aR,11S,12aS,14aR,14bS)-3-(Hydroxymethyl)-5-(methoxymethoxy)-11-(((3aR,4R,6S,7S,7aR)-7-(methoxymethoxy)-2,2,6-trimethyltetrahydro-4H-[1,3]dioxolo[4,5-c]pyran-4-yl)oxy)-3a,8,8-trimethyltetradecahydro-6H-cyclopenta[7,8]

phenanthro[4,4a-d][1,3]dioxine-12a,14b-diol (10). Aldehyde **4** (0.500 g, 0.716 mmol) was dissolved in methanol (10 mL), and the mixture was cooled to 0 °C. Solid sodium borohydride (0.0816 g, 2.14 mmol) was added, and the reaction mixture was stirred for 30 min. The reaction was quenched with a saturated aqueous NH₄Cl (15 mL) solution and extracted with ethyl acetate (3 × 15 mL). The organic layers were combined, dried over Na₂SO₄, and filtered, and the volatiles were removed under reduced pressure. The resultant residue was purified by column chromatography (silica gel, hexanes/ethyl acetate, 2:8) to afford the corresponding alcohol **10** (0.391 g, 78%) as a white solid: mp 126−129 °C; $[\alpha]_D^{22}$ −4.12 (c 1.55, CHCl₃); ¹H NMR (400 MHz, CDCl₃) δ 5.11 (s, 1H), 4.96 (d, J = 6.4 Hz, 1H), 4.92 (t, J = 3.2 Hz, 1H), 4.82 (d, J = 6.5 Hz, 1H), 4.69−4.62 (m, 3H), 4.44 (d, J = 12.3 Hz, 1H), 4.17−4.08 (m, 2H), 4.07 (d, J = 5.5 Hz, 1H), 3.95 (dq, J = 12.5, 6.2 Hz, 1H), 3.89−3.70 (m, 3H), 3.51 (dd, J = 10.8, 2.9 Hz, 1H), 3.44−3.36 (m, 4H), 3.35 (s, 3H), 2.11−1.88 (m, 7H), 1.87−1.73 (m, 3H), 1.65−1.20 (m, 23H), 1.16−0.98 (m, 4H); ¹³C NMR (100 MHz, CDCl₃) δ 109.1, 100.8, 97.5, 96.7, 96.3, 82.1, 78.3, 78.2, 76.5, 73.2, 73.0, 66.9, 64.6, 62.2, 60.6, 55.89, 55.85, 50.7, 47.8, 47.2, 46.7, 45.3, 40.1, 36.3, 34.9, 32.8, 30.3, 27.9, 26.5, 24.9, 23.1, 21.6, 17.5, 15.5; HRMS (ESI) calcd for $C_{36}H_{61}O_{13}$ [M + H]⁺ 701.4112, found 701.4091.

(3S,3aR,5R,5aS,5bR,9aR,11S,12aS,14aR,14bS)-12a,14b-Dihydroxy-5-(methoxymethoxy)-11-(((3aR,4R,6S,7S,7aR)-7-(methoxymethoxy)-2,2,6-trimethyltetrahydro-4H-[1,3]dioxolo[4,5-c]pyran-4-yl)oxy)-3a,8,8-trimethylhexadecahydro-6H-cyclopenta[7,8]-phenanthro[4,4a-d][1,3]dioxine-3-carbonitrile (11). To a solution of aldehyde **4** (0.250 g, 0.357 mmol) in EtOH (10 mL) at room temperature were added NH₂OH·HCl (0.100 g, 1.43 mmol) and NaOAc (0.131 g, 1.60 mmol). After stirring for 1 h, the reaction mixture was diluted with water (10 mL) and extracted with EtOAc (3 × 10 mL). The combined organic layers were dried over Na₂SO₄ and concentrated under reduced pressure to give the corresponding oxime (0.240 g) as a white foam.

To a stirred solution of the above oxime (0.240 g, 0.336 mmol) in CH₂Cl₂ (20 mL) was added 1,1′-carbonyldiimidazole (0.190 g, 1.17 mmol) at room temperature. After the mixture was stirred for 12 h, saturated aqueous NH₄Cl (10 mL) was added to the reaction mixture, and then the mixture was extracted with CH₂Cl₂ (3 × 15 mL). The combined organic extracts were dried over Na₂SO₄ and concentrated under reduced pressure to form a residue, which was purified by column chromatography (silica gel, hexanes/ethyl acetate, 7:3) to furnish nitrile **11** (0.173 g, 70%) as a white solid: mp 97−99 °C; $[\alpha]_D^{22}$ −7.24 (c 0.276, CHCl₃); ¹H NMR (400 MHz, CDCl₃) δ 5.07 (d, J = 22.9 Hz, 1H), 4.96 (d, J = 6.3 Hz, 1H), 4.81−4.55 (m, 4H), 4.46 (d, J = 12.2 Hz, 1H), 4.19−4.02 (m, 3H), 3.95 (dd, J = 14.0, 7.5 Hz, 2H), 3.65 (d, J = 12.3 Hz, 1H), 3.47−3.26 (m, 7H), 2.84 (t, J = 7.1 Hz, 1H), 2.24−1.65 (m, 11H), 1.50 (d, J = 18.8 Hz, 6H), 1.42−1.17 (m, 16H), 1.12−0.91 (m, 3H); ¹³C NMR (100 MHz, CDCl₃) δ 121.7, 109.1, 100.9, 97.1, 96.8, 96.3, 83.1, 78.3, 78.1, 76.5, 75.6, 72.9, 66.6, 64.6, 60.5, 56.1, 55.8, 47.54, 47.45, 45.3, 41.8, 40.4, 39.4, 35.8, 34.7, 33.2, 30.3, 27.9, 26.4, 25.6, 24.8, 23.0, 22.6, 19.1, 18.0, 17.5; HRMS (ESI) calcd for $C_{36}H_{58}O_{12}$ [M + H]⁺ 696.3959, found 696.3949.

4-((3R,3aR,5R,5aS,5bR,9aR,11S,12aS,14aR,14bS)-5,11,12a,14b-Tetrahydroxy-3a,8,8-trimethylhexadecahydro-6H-cyclopenta[7,8]-phenanthro[4,4a-d][1,3]dioxin-3-yl)furan-2(5H)-one (12). Ouabain octahydrate (10.0 g, 13.7 mmol) was suspended in acetone (500 mL) containing concentrated hydrochloric acid (5.00 mL). After the mixture was stirred at ambient temperature for 5 days, a white solid of **12** had precipitated. The solid was filtered off, washed with acetone, and dried under reduced pressure to give **12** (3.60 g, 55%) Acetonide **12** was pure enough to use for the next step without further purification: mp 245−247 °C; ¹H NMR (400 MHz, DMSO-d₆) δ 5.93 (d, J = 1.8 Hz, 1H), 5.08 (t, J = 3.1 Hz, 1H), 4.93−4.84 (m, 3H), 4.79 (d, J = 3.3 Hz, 1H), 4.48 (d, J = 5.2 Hz, 1H), 4.27 (d, J = 11.9 Hz, 1H), 4.16 (s, 1H), 4.09−4.03 (m, 1H), 3.95 (tt, J = 8.5, 5.1 Hz, 1H), 3.63 (d, J = 11.9 Hz, 1H), 3.00 (t, J = 7.4 Hz, 1H), 2.08−1.73 (m, 7H), 1.65−1.18 (m, 14H), 1.07−0.88 (m, 1H), 0.75 (s, 3H) ; ¹³C NMR (100 MHz, DMSO-d₆) δ 174.9, 173.7, 115.9, 99.3, 82.4, 73.17, 73.11, 66.6, 65.6, 65.3, 60.2, 48.9, 48.3, 46.8, 46.3, 45.7, 36.8, 36.5, 32.9, 31.7,

30.6, 25.9, 24.4, 23.9, 22.4, 17.5; HRMS (ESI) calcd for $C_{26}H_{39}O_8$ [M + H]$^+$ 479.2645, found 479.2641.

4-((3R,3aR,5R,5aS,5bR,9aR,11S,12aS,14aR,14bS)-12a-Hydroxy-5,11,14b-tris(methoxymethoxy)-3a,8,8-trimethylhexadecahydro-6H-cyclopenta[7,8]phenanthro[4,4a-d][1,3]dioxin-3-yl)furan-2(5H)-one (13). To a suspension of **12** (0.990 g, 2.07 mmol) in CH_2Cl_2 (30 mL) was added diisopropylethylamine (3.61 mL, 20.7 mmol) at room temperature. After stirring for 5 min, the reaction mixture was cooled to 0 °C, and chloromethyl methyl ether (MOM-Cl) (0.937 mL, 12.4 mmol) was added. The mixture was warmed to room temperature and stirred for 72 h, and then the reaction mixture was diluted with water (30 mL). The organic phase was separated, and the aqueous phase was extracted with additional CH_2Cl_2 (2 × 30 mL). The combined organic layers were dried over Na_2SO_4 and concentrated under reduced pressure. The residue was purified by column chromatography (silica gel, hexanes/ethyl acetate 1:9) to give **13** (0.983 g, 75%) as a yellow foam: ^1H NMR (400 MHz, CDCl$_3$) δ 5.86 (d, *J* = 1.2 Hz, 1H), 4.92−4.47 (m, 10H), 4.35 (d, *J* = 12.9 Hz, 2H), 4.12 (s, 1H), 3.58 (d, *J* = 12.2 Hz, 1H), 3.49−3.28 (m, 10H), 2.20−1.70 (m, 11H), 1.63−1.23 (m, 10H), 1.21−1.05 (m, 1H), 0.75 (s, 3H); ^{13}C NMR (100 MHz, CDCl$_3$) δ 173.9, 170.9, 116.8, 101.2, 95.8, 94.7, 92.7, 90.6, 74.7, 73.5, 72.5, 70.8, 66.4, 60.8, 56.3, 56.1, 55.6, 48.3, 47.3, 46.6, 43.7, 40.6, 38.6, 34.9, 34.5, 30.2, 29.6, 27.9, 25.2, 23.1, 21.9, 20.9; HRMS (ESI) calcd for $C_{32}H_{50}O_{11}$Na [M + Na]$^+$ 633.3251, found 633.3261.

2-Hydroxy-1-((3S,3aR,5R,5aS,5bR,9aR,11S,12aS,14aR,14bS)-12a-hydroxy-5,11,14b-tris(methoxymethoxy)-3a,8,8-trimethylhexadecahydro-6H-cyclopenta[7,8]phenanthro[4,4a-d][1,3]dioxin-3-yl)-ethan-1-one (14). Ozone was bubbled through a solution of **13** (0.965 g, 1.58 mmol) in CH_2Cl_2 (20 mL) at −78 °C for 1 h. Once the deep blue color persisted, the reaction was allowed to stir at −78 °C for 2 h. Excess ozone was removed by bubbling N_2 through the solution until the solution became colorless. Zn (5.65 g, 87.0 mmol) and AcOH (5.88 mL, 103 mmol) were added to the above solution, and the mixture was stirred for 2 h at room temperature. The suspension was filtered through a pad of Celite, and the pad was washed with CH_2Cl_2 (60 mL). The filtrate was washed with water (30 mL) and brine (30 mL), dried over Na_2SO_4, and concentrated under reduced pressure to afford the desired hydroxymethyl ester (1.03 g), which was used for the next step without further purification.

To a solution of the hydroxymethyl ester (1.00 g, 1.55 mmol) in methanol (20 mL) was added KHCO$_3$ (0.465 g, 4.65 mmol) in water (1 mL). After the mixture was stirred at room temperature for 3 h, the methanol was removed under reduced pressure. The residue was taken up in EtOAc (50 mL), and the mixture was washed with water (30 mL). The organic layer was dried over Na_2SO_4 and concentrated under reduced pressure to afford the unstable hydroxymethyl ketone **14**. The residue was passed through a short silica gel plug (10 g silica gel, hexanes/ethyl acetate, 1:1) to give **14** (0.618 g) as a white foam in 63% yield over two steps, which was used for the next step without further characterization.

(R)-1-((3S,3aR,5R,5aS,5bR,9aR,11S,12aS,14aR,14bS)-12a-Hydroxy-5,11,14b-tris(methoxymethoxy)-3a,8,8-trimethylhexadecahydro-6H-cyclopenta[7,8]phenanthro[4,4a-d][1,3]dioxin-3-yl)ethane-1,2-diol and (S)-1-((3S,3aR,5R,5aS,5bR,9aR,11S,12aS,14aR,14bS)-12a-Hydroxy-5,11,14b-tris(methoxymethoxy)-3a,8,8-trimethylhexadecahydro-6H-cyclopenta[7,8]phenanthro[4,4a-d][1,3]dioxin-3-yl)-ethane-1,2-diol (15). To a solution of hydroxymethyl ketone **14** (1.00 g, 1.70 mmol) in methanol (20 mL) was added solid sodium borohydride (0.194 g, 5.11 mmol) at 0 °C. After stirring for 30 min, the reaction was quenched with saturated aqueous NH$_4$Cl (20 mL). The resultant mixture was extracted with ethyl acetate (3 × 30 mL). The combined organic layers were dried over Na_2SO_4 and concentrated under reduced pressure. The residue was purified by column chromatography (silica gel, hexanes/ethyl acetate 1:9) to afford a diastereomeric mixture of diol **15** (0.762 g, 76%) as a white foam: ^1H NMR (400 MHz, CDCl$_3$) δ 4.90−4.53 (m, 8H), 4.48 (d, *J* = 12.2 Hz, 1H), 4.09−3.60 (m, 4H), 3.59−3.21 (m, 11H), 2.31−1.18 (m, 24H), 1.19−0.97 (s, 4H); ^{13}C NMR (100 MHz, CDCl$_3$) δ 100.9, 97.1, 94.6, 91.8, 91.4, 75.6, 72.8, 70.8, 69.6, 66.9, 66.3, 60.8, 56.2, 56.0, 55.5, 50.9, 48.7, 48.1, 46.4, 46.1, 38.1, 36.4, 35.1, 30.4, 29.3, 25.0, 23.7,

23.1, 19.3, 17.6; HRMS (ESI) calcd for $C_{30}H_{53}O_{11}$ [M + H]$^+$ 589.3588, found 589.3569.

(3S,3aR,5R,5aS,5bR,9aR,11S,12aS,14aR,14bS)-12a-Hydroxy-5,11,14b-tris(methoxymethoxy)-3a,8,8-trimethylhexadecahydro-6H-cyclopenta[7,8]phenanthro[4,4a-d][1,3]dioxine-3-carbaldehyde (16). To a solution of diol **15** (0.650 g, 1.10 mmol) in THF/H_2O (8:2) (20 mL) was added sodium periodate (0.706 g, 3.31 mmol) at ambient temperature. After the mixture was stirred for 1 h, the white precipitate was filtered off and the filtrate was diluted with water (20 mL). The mixture was extracted with ethyl acetate (3 × 20 mL), and the combined organic layers were dried over Na_2SO_4 and filtered. The solvent was then removed under reduced pressure. The residue was purified by column chromatography (silica gel, hexanes/ethyl acetate, 7:3) to afford aldehyde **16** (0.381 g, 62%) as a white solid: mp 129−135 °C; ^1H NMR (400 MHz, CDCl$_3$) δ 9.66 (d, *J* = 2.2 Hz, 1H), 4.90−4.32 (m, 9H), 4.23−3.94 (m, 2H), 3.78−3.54 (m, 1H), 3.51−3.13 (m, 9H), 2.56 (dd, *J* = 9.7, 3.7 Hz, 1H), 2.10−1.65 (m, 11H), 1.51−1.28 (m, 10H), 1.12−0.88 (m, 4H); ^{13}C NMR (100 MHz, CDCl$_3$) δ 204.3, 100.9, 96.8, 94.6, 92.2, 89.9, 75.2, 72.7, 70.8, 66.7, 60.7, 59.8, 56.1, 55.92, 55.52, 50.3, 47.8, 45.3, 43.1, 39.5, 35.9, 34.8, 29.4, 28.2, 25.0, 23.1, 22.9, 20.9, 17.8; HRMS (ESI) calcd for $C_{29}H_{48}O_{10}$ Na [M + Na]$^+$ 579.3145, found 579.3118.

(3S,3aR,5R,5aS,5bR,9aR,11S,12aS,14aR,14bS)-3-(Hydroxymethyl)-5,11,14b-tris(methoxymethoxy)-3a,8,8-trimethyltetradecahydro-6H-cyclopenta[7,8]phenanthro[4,4a-d][1,3]dioxin-12a(1H)-ol (17). To a solution of aldehyde **16** (0.50 g, 0.89 mmol) in methanol (10 mL) at 0 °C was added solid sodium borohydride (0.10 g, 2.7 mmol). After stirring for 30 min, the reaction was quenched with saturated aqueous NH$_4$Cl (15 mL) and extracted with ethyl acetate (3 × 15 mL). The organic layers were combined, dried over Na_2SO_4, and filtered, and the solvent was removed under reduced pressure. The resultant residue was purified by column chromatography (silica gel, hexanes/ethyl acetate, 1:1) to afford alcohol **17** (0.36 g, 72%) as a white solid: mp 154−158 °C; [α]$_D^{22}$ +2.68 (*c* 1.30, CHCl$_3$); ^1H NMR (400 MHz, CDCl$_3$) δ 4.79−4.69 (m, 5H), 4.70−4.60 (m, 2H), 4.51 (dd, *J* = 7.4, 4.4 Hz, 2H), 4.12 (dt, *J* = 12.1, 6.4 Hz, 2H), 3.72−3.56 (m, 2H), 3.42 (s, 3H), 3.40 (s, 3H), 3.39 (s, 3H), 2.33 (td, *J* = 12.8, 6.3 Hz, 1H), 2.21 (d, *J* = 18.8 Hz, 1H), 2.19−2.07 (m, 2H), 2.06−1.94 (m, 2H), 1.95−1.73 (m, 5H), 1.74−1.62 (m, 1H), 1.63−1.30 (m, 12H), 1.24−1.04 (m, 1H), 0.94 (s, 3H); ^{13}C NMR (100 MHz, CDCl$_3$) δ 100.9, 96.6, 94.6, 92.4, 91.5, 76.0, 72.7, 70.9, 66.7, 63.6, 60.8, 56.0, 55.9, 55.5, 49.1, 47.5, 47.2, 44.3, 41.4, 39.8, 35.4, 34.6, 29.9, 29.4, 25.7, 25.1, 23.1, 22.4, 18.0; HRMS (ESI) calcd for $C_{29}H_{50}O_{10}$Na [M + Na]$^+$ 581.3302, found 581.3282.

(3S,3aR,5R,5aS,5bR,9aR,11S,12aS,14aR,14bS)-3-(Azidomethyl)-5,11,14b-tris(methoxymethoxy)-3a,8,8-trimethyltetradecahydro-6H-cyclopenta[7,8]phenanthro[4,4a-d][1,3]dioxin-12a(1H)-ol (18). To a solution of alcohol **17** (0.10 g, 0.17 mmol) in CH_2Cl_2/pyridine (5:1, 6 mL) at 0 °C was added TsCl (0.051 g, 0.26 mmol). The reaction mixture was stirred at ambient temperature for 6 h, and then the reaction mixture was poured into water and extracted with CH_2Cl_2 (3 × 10 mL). The combined organic layers were dried over Na_2SO_4 and concentrated under reduced pressure. The residue was purified by column chromatography (silica gel, hexanes/ethyl acetate, 8:2) to give the required tosylate (0.090 g, 73%) as a colorless oil: ^1H NMR (400 MHz, CDCl$_3$) δ 7.77 (d, *J* = 8.3 Hz, 2H), 7.33 (d, *J* = 8.2 Hz, 2H), 4.77−4.50 (m, 7H), 4.51−4.38 (m, 1H), 4.20−3.99 (m, 3H), 3.92 (t, *J* = 8.6 Hz, 1H), 3.57 (dd, *J* = 20.2, 12.6 Hz, 1H), 3.41−3.33 (m, 3H), 3.31 (s, 3H), 3.29 (s, 3H), 2.55−2.38 (m, 4H), 2.18−1.87 (m, 4H), 1.87−1.64 (m, 5H), 1.62−1.48 (m, 1H), 1.49−1.17 (m, 12H), 1.12−0.95 (m, 1H), 0.74 (s, 3H).

To a stirred solution of the above tosylate (0.50 g, 0.70 mmol) in DMSO (10 mL) was added NaN$_3$ (0.13 g, 2.1 mmol), and the resultant reaction mixture was heated at 60 °C for 2.5 h. The reaction mixture was diluted with water (15 mL) and extracted with Et$_2$O (3 × 15 mL). The combined ether layers were washed with brine (15 mL), dried over Na_2SO_4, and concentrated under reduced pressure. The residue was purified by column chromatography (silica gel, hexanes/ethyl acetate, 8:2) to afford azide **18** (0.28 g, 70%) as a yellow liquid: ^1H NMR (400 MHz, CDCl$_3$) δ 4.79−4.55 (m, 7H), 4.57−4.40 (m, 2H), 4.19 (t, *J* = 13.1 Hz, 1H), 4.11 (s, 1H), 3.71−3.51 (m, 1H),

3.46−3.29 (m, 10H), 3.22−3.06 (m, 1H), 2.35 (tt, J = 9.8, 6.6 Hz, 1H), 2.15−1.86 (m, 5H), 1.77 (ddd, J = 22.5, 9.8, 5.3 Hz, 4H), 1.67−1.54 (m, 1H), 1.51−1.27 (m, 11H), 1.12 (dd, J = 23.8, 10.7 Hz, 1H), 0.82 (s, 3H).

(1R,3S,5S,8R,9S,10R,11R,13R,14S,17S)-10-(Hydroxymethyl)-17-((4-(4-methoxyphenyl)-1H-1,2,3-triazol-1-yl)methyl)-13-methyltetradecahydro-5H-cyclopenta[a]phenanthrene-1,3,5,11,14(2H)-pentaol (19). To a solution of azide **18** (0.076 g, 0.13 mmol) and 4-methoxyphenyl acetylene (0.025 g, 0.19 mmol) in DMF (2 mL) was added sodium ascorbate (0.010 g, 0.052 mmol) in water (1 mL), and the reaction mixture was stirred for 2 min. Then CuSO$_4$·5H$_2$O (0.0064 g, 0.026 mmol) in water (1 mL) was added. After the mixture was stirred at room temperature for 12 h, water (4 mL) was added. Extraction with EtOAc (3 × 5 mL), followed by removal of the combined organic extracts under reduced pressure, afforded a green solid, which was purified by column chromatography (hexanes/ethyl acetate, 3:7) to give the triazole intermediate (0.063 g, 68%) as a white foam: ^{1}H NMR (400 MHz, CDCl$_3$) δ 7.75−7.70 (m, 3H), 7.05−6.84 (m, 2H), 4.81−4.65 (m, 6H), 4.54−4.44 (m, 2H), 4.40 (dd, J = 13.3, 3.8 Hz, 1H), 4.34−4.17 (m, 2H), 4.12−4.08 (m, 1H), 3.84 (s, 3H), 3.75−3.58 (m, 1H), 3.43−3.34 (m, 9H), 2.77−2.62 (m, 1H), 2.16−1.87 (m, 4H), 1.86−1.57 (m, 6H), 1.56−1.27 (m, 12H), 1.09 (dd, J = 19.8, 7.4 Hz, 1H), 0.97 (s, 3H); ^{13}C NMR (100 MHz, CDCl$_3$) δ 159.5, 147.5, 126.8, 123.5, 119.0, 114.2, 101.0, 96.2, 94.7, 92.8, 91.0, 74.9, 72.6, 70.9, 66.6, 60.8, 56.2, 55.9, 55.5, 55.3, 51.7, 47.5, 47.4, 47.3, 44.0, 40.4, 39.4, 35.2, 34.5, 29.5, 28.9, 27.0, 25.1, 23.1, 22.1, 18.2.

The triazole intermediate (0.050 g, 0.069 mmol) was dissolved in 4 N HCl in MeOH (5 mL), and the solution was stirred at room temperature for 12 h. After completion of the reaction (monitored by TLC), the solvent was removed under reduced pressure. The residue was purified by column chromatography (silica gel, EtOAc/MeOH, 8:2 with 2% water) to give **19** (0.019 g, 51%) as a white foam: $[\alpha]_D^{22}$ +13.7 (*c* 0.241, MeOH); ^{1}H NMR (400 MHz, CD$_3$OD) δ 8.59 (s, 1H), 7.72 (d, J = 8.4 Hz, 2H), 7.03 (d, J = 8.3 Hz, 2H), 4.70−4.54 (m, 3H), 4.47−3.98 (m, 4H), 3.82 (s, 3H), 2.42−1.17 (m, 20H (overlap with grease)); HRMS (ESI) calcd for C$_{29}$H$_{42}$N$_3$O$_7$ [M + H]$^+$ 544.3023, found 544.3035.

(3R,3aR,5R,5aS,5bR,9aR,11S,12aS,14aR,14bS)-3-Ethynyl-5,11,14b-tris(methoxymethoxy)-3a,8,8-trimethyltetradecahydro-6H-cyclopenta[7,8]phenanthro[4,4a-d][1,3]dioxin-12a(1H)-ol (21). To a solution of **20** (0.103 g, 0.539 mmol) in methanol (3 mL) was added K$_2$CO$_3$ (0.148 g, 1.07 mmol), and the mixture was stirred for 5 min. A solution of aldehyde **16** (0.200 g, 0.359 mmol) in MeOH (2 mL) was added to the above mixture at 0 °C. After stirring at room temperature for 3 h, the reaction mixture was diluted with water (10 mL), extracted with EtOAc (3 × 10 mL), washed with brine (10 mL), dried over Na$_2$SO$_4$, filtered, and concentrated under reduced pressure. Purification by flash chromatography (silica gel, acetone/hexanes, 9:1) gave alkyne **21** (0.140 g, 71%) as a yellow foam: ^{1}H NMR (400 MHz, CDCl$_3$) δ 5.09−4.36 (m, 9H), 4.09 (s, 1H), 3.77 (dd, J = 16.6, 10.3 Hz, 2H), 3.51−3.25 (m, 9H), 2.71 (d, J = 5.1 Hz, 1H), 2.30−1.59 (m, 11H), 1.60−1.17 (m, 11H), 1.17−0.88 (m, 4H); ^{13}C NMR (100 MHz, CDCl$_3$) δ 100.9, 97.3, 94.6, 92.7, 89.9, 84.6, 76.0, 72.9, 70.8, 70.4, 66.9, 60.5, 56.0, 55.8, 55.5, 48.8, 48.0, 45.9, 40.6, 40.0, 38.9, 36.2, 35.0, 29.3, 27.4, 25.3, 25.0, 23.1, 22.8, 17.6; HRMS (ESI) calcd for C$_{30}$H$_{49}$O$_9$ [M + H]$^+$ 553.3377, found 553.3359.

(3S,3aR,5R,5aS,5bR,9aR,11S,12aS,14aR,14bS)-3-(1-Benzyl-1H-1,2,3-triazol-4-yl)-5,11,14b-tris(methoxymethoxy)-3a,8,8-trimethyltetradecahydro-6H-cyclopenta[7,8]phenanthro[4,4a-d][1,3]dioxin-12a(1H)-ol (22). To a stirred solution of benzyl azide (0.049 g, 0.38 mmol) and alkyne **21** (0.14 g, 0.25 mmol) in DMF (2 mL) was added sodium ascorbate (0.024 g, 0.10 mmol) in water (1 mL). After the mixture was stirred for 2 min, CuSO$_4$·5H$_2$O (0.012 g, 0.050 mmol) in water (1 mL) was added to the reaction. The mixture was stirred at room temperature for 12 h; then water (5 mL) was added, and the reaction mixture was extracted with EtOAc (3 × 10 mL). Evaporation of the combined organic extracts under reduced pressure afforded a green solid, which was purified by flash column chromatography (hexanes/acetone, 7:3) to give compound **22** (0.099 g, 58%) as a white foam: $[\alpha]_D^{22}$ +32.3 (*c* 0.257, CHCl$_3$); ^{1}H NMR (400 MHz, CDCl$_3$) δ 7.39−7.29 (m, 3H), 7.25−7.19 (m, 2H), 7.18 (s, 1H), 5.49

(q, J = 14.9 Hz, 2H), 4.91 (t, J = 3.3 Hz, 1H), 4.82 (d, J = 7.5 Hz, 1H), 4.76−4.64 (m, 5H), 4.53 (t, J = 7.1 Hz, 1H), 4.42 (d, J = 12.2 Hz, 1H), 4.08 (s, 1H), 3.68 (ddd, J = 13.6, 10.8, 6.1 Hz, 2H), 3.38 (d, J = 2.8 Hz, 6H), 3.29−3.17 (m, 1H), 3.09 (s, 3H), 2.25−1.90 (m, 7H), 1.87−1.65 (m, 3H), 1.60−1.40 (m, 3H), 1.40−1.29 (m, 6H), 1.26 (m, 3H), 1.02 (s, 3H); ^{13}C NMR (100 MHz, CDCl$_3$) δ 147.7, 134.9, 129.0, 128.6, 127.8, 121.1, 100.9, 97.3, 94.6, 93.0, 91.1, 76.4, 73.0, 70.8, 66.9, 60.4, 56.1, 55.5, 54.0, 48.71, 48.01, 45.8, 45.7, 40.6, 39.2, 36.2, 34.9, 29.6, 25.81, 25.14, 25.01, 23.0, 22.8, 18.23; HRMS (ESI) calcd for C$_{37}$H$_{56}$N$_3$O$_9$ [M + H]$^+$ 686.4017, found 686.4005.

(3S,3aR,5R,5aS,5bR,9aR,11S,12aS,14aR,14bS)-3-(1-(4-Chlorobenzyl)-1H-1,2,3-triazol-4-yl)-5,11,14b-tris(methoxymethoxy)-3a,8,8-trimethyltetradecahydro-6H-cyclopenta[7,8]phenanthro[4,4a-d][1,3]-dioxin-12a(1H)-ol (23). The procedure described for the synthesis of **22** was followed to obtain compound **23** (0.14 g, 56%) as a white foam: ^{1}H NMR (400 MHz, CDCl$_3$) δ 7.38−7.28 (m, 2H), 7.22−7.09 (m, 3H), 5.46 (q, J = 15.1 Hz, 2H), 4.91 (t, J = 3.2 Hz, 1H), 4.83 (d, J = 7.5 Hz, 1H), 4.73 (t, J = 3.4 Hz, 2H), 4.71−4.65 (m, 3H), 4.53 (d, J = 6.4 Hz, 1H), 4.43 (d, J = 12.2 Hz, 1H), 4.15−4.02 (m, 1H), 3.69 (ddd, J = 13.1, 10.9, 5.6 Hz, 2H), 3.38 (t, J = 4.4 Hz, 6H), 3.31−3.18 (m, 1H), 3.11 (s, 3H), 2.15−1.91 (m, 6H), 1.84−1.66 (m, 2H), 1.61−1.41 (m, 3H), 1.40−1.27 (m, 6H), 1.26−1.24 (m, 5H), 1.00 (s, 3H); ^{13}C NMR (100 MHz, CDCl$_3$) δ 147.9, 134.7, 133.4, 129.30, 129.17, 121.1, 100.9, 97.3, 94.6, 93.0, 91.0, 76.4, 73.0, 70.8, 66.9, 60.4, 56.1, 55.5, 53.2, 48.7, 48.0, 45.8, 45.7, 40.6, 39.2, 36.2, 35.0, 29.3, 25.7, 25.1, 25.0, 23.1, 22.8, 18.2; HRMS (ESI) calcd for C$_{37}$H$_{55}$N$_3$O$_9$ Cl [M + H]$^+$ 720.3627, found 720.3644.

(3S,3aR,5R,5aS,5bR,9aR,11S,12aS,14aR,14bS)-3-(1-(4-Fluorobenzyl)-1H-1,2,3-triazol-4-yl)-5,11,14b-tris(methoxymethoxy)-3a,8,8-trimethyltetradecahydro-6H-cyclopenta[7,8]phenanthro[4,4a-d][1,3]-dioxin-12a(1H)-ol (24). The procedure described for the synthesis of **22** was followed to obtain compound **24** (0.15 g, 66%) as a white foam: ^{1}H NMR (400 MHz, CDCl$_3$) δ 7.25−7.12 (m, 3H), 7.03 (t, J = 8.6 Hz, 2H), 5.45 (q, J = 15.2 Hz, 2H), 4.94−4.86 (m, 1H), 4.82 (t, J = 8.3 Hz, 1H), 4.76−4.63 (m, 5H), 4.59−4.37 (m, 2H), 4.10−4.03 (m, 1H), 3.69−3.58 (m, 2H), 3.36−3.09 (m, 10H), 2.22−1.87 (m, 6H overlapped with solvent acetone), 1.86−1.63 (m, 3H), 1.56−1.28 (m, 10H), 1.24 (d, J = 4.7 Hz, 3H), 1.07−0.95 (m, 2.25H), 0.44 (s, 0.75H).

(1R,3S,5S,8R,9S,10R,11R,13R,14S,17S)-17-(1-Benzyl-1H-1,2,3-triazol-4-yl)-10-(hydroxymethyl)-13-methyltetradecahydro-5H-cyclopenta[a]phenanthrene-1,3,5,11,14(2H)-pentaol (25). Compound **22** (0.050 g, 0.072 mmol) was dissolved in 4 N HCl in MeOH (5 mL), and the solution was stirred at room temperature for 12 h. After completion of the reaction, the solvent was removed under reduced pressure. The residue was purified by column chromatography on silica gel (EtOAc/MeOH, 8:2 with 2% water) to give **25** (0.017 g, 47%) as a white solid: mp 109−111 °C; $[\alpha]_D^{22}$ −36.7 (*c* 0.248, MeOH); ^{1}H NMR (400 MHz, CD$_3$OD) δ 7.81 (s, 1H), 7.47−7.19 (m, 5H), 5.58 (s, 2H), 4.51−3.95 (m, 4H), 3.51−3.37 (m, 1H), 2.12 (m 7H), 1.84−1.17 (m, 9H), 1.10−0.80 (m, 4H); ^{13}C NMR (100 MHz, CD$_3$OD) δ 148.6, 136.4, 130.1, 129.77, 129.10, 125.0, 87.3, 78.7, 78.4, 75.8, 68.6, 62.7, 55.4, 52.3, 50.0, 47.1, 39.0, 38.9, 38.2, 37.4, 37.0, 31.5, 26.0, 25.3, 21.4, 19.6; HRMS (ESI) calcd for C$_{28}$H$_{40}$N$_3$O$_6$ [M + H]$^+$ 514.2917, found 514.2908.

(1R,3S,5S,8R,9S,10R,11R,13R,14S,17S)-17-(1-(4-Chlorobenzyl)-1H-1,2,3-triazol-4-yl)-10-(hydroxymethyl)-13-methyltetradecahydro-5H-cyclopenta[a]phenanthrene-1,3,5,11,14(2H)-pentaol (26). The procedure described for the synthesis of **25** was followed to obtain compound **26** (0.027 g, 51%) as a white foam: ^{1}H NMR (400 MHz, CD$_3$OD) δ 8.26−8.08 (m, 1H), 7.39 (dd, J = 21.4, 8.5 Hz, 4H (overlapped with EtOAc)), 5.66 (d, J = 9.0 Hz, 2H), 4.45−4.11 (m, 4H), 3.56−3.39 (m, 1H), 2.38−2.03 (m, 7H (overlapped with EtOAc)), 1.82−1.24 (m, 9H), 1.11−0.79 (m, 4H); HRMS (ESI) calcd for C$_{28}$H$_{39}$ClN$_3$O$_6$Na [M + Na]$^+$ 570.2346, found 570.2349.

(1R,3S,5S,8R,9S,10R,11R,13R,14S,17S)-17-(1-(4-Fluorobenzyl)-1H-1,2,3-triazol-4-yl)-10-(hydroxymethyl)-13-methyltetradecahydro-5H-cyclopenta[a]phenanthrene-1,3,5,11,14(2H)-pentaol (27). The procedure described for the synthesis of **25** was followed to obtain compound **27** (0.040 g, 53%) as a white solid: mp 166−168 °C; $[\alpha]_D^{22}$ −6.25 (*c* 0.288, MeOH); ^{1}H NMR (400 MHz, CD$_3$OD) δ 7.83−7.74

(s, 0.7 H), 7.67 (s, 0.3H), 7.42−7.21 (m, 2H), 7.09 (dd, J = 12.2, 5.2 Hz, 2H), 5.60−5.38 (m, 2H), 4.47−3.84 (m, 4H), 3.49−3.35 (m, 1H), 2.37−1.48 (m, 13H), 1.35−1.29 (m, 3H), 1.05−0.91 (m, 3H), 0.67 (s, 1H); ^{13}C NMR (100 MHz, CD$_3$OD) δ 165.3, 162.9, 154.0, 149.4, 133.17, 133.14, 131.1, 131.0, 124.3, 123.9, 116.8, 116.6, 87.5, 86.4, 78.7, 77.5, 73.1, 68.9, 62.3, 54.0, 50.1, 46.7, 42.31, 40.9, 33.8, 31.8, 30.7, 29.9, 25.8, 24.1, 23.6, 18.9, 17.8; HRMS (ESI) calcd for C$_{28}$H$_{39}$FN$_3$O$_6$ [M + H]$^+$ 532.2823, found 532.2807.

(E)-12a-Hydroxy-5,11,14b-tris(methoxymethyl)-3a,8,8-trimethylhexadecahydro-6H-cyclopenta[7,8]phenanthro[4,4a-d][1,3]-dioxine-3-carbaldehyde Oxime and (Z)-12a-Hydroxy-5,11,14b-tris-(methoxymethoxy)-3a,8,8-trimethylhexadecahydro-6H-cyclopenta-[7,8]phenanthro[4,4a-d][1,3]dioxine-3-carbaldehyde Oxime (28). To a solution of aldehyde **16** (0.600 g, 1.07 mmol) in EtOH (10 mL) at room temperature were added NH$_2$OH·HCl (0.297 g, 4.31 mmol) and NaOAc (0.398 g, 4.85 mmol). After stirring for 1 h, the reaction mixture was diluted with water (15 mL) and extracted with EtOAc (3 × 15 mL). The combined organic layers were dried over Na$_2$SO$_4$ and concentrated under reduced pressure. The residue was purified by column chromatography (silica gel, hexanes/ethyl acetate, 7:3) to give aldoxime **28** (0.499 g, 81%) as a white foam: $[\alpha]_D^{22}$ +17.6 (c 0.847, CHCl$_3$); ^{1}H NMR (400 MHz, CDCl$_3$) δ 7.39 (dd, J = 14.0, 7.3 Hz, 0.7H), 6.81 (d, J = 7.7 Hz, 0.3H), 4.79−4.63 (m, 7H), 4.57 (d, J = 13.2 Hz, 1H), 4.54−4.42 (m, 1H), 4.23−3.95 (m, 2H), 3.74−3.59 (m, 1H), 3.42−3.31 (m, 9H), 2.89 (dd, J = 15.6, 7.8 Hz, 1H), 2.15−1.28 (m, 22H), 1.14−0.95 (m, 2H), 0.91−0.81 (m, 2H); ^{13}C NMR (100 MHz, CDCl$_3$) δ 154.1, 101.0, 100.9, 96.6, 95.9, 94.6, 92.5, 92.3, 90.7, 90.5, 74.9, 74.6, 72.9, 72.8, 70.9, 66.8, 66.6, 60.8, 56.3, 56.2, 55.96, 55.90, 55.57, 55.54, 49.5, 48.9, 47.5, 45.6, 44.4, 43.5, 40.2, 39.4, 35.4, 34.9, 34.6, 29.5, 26.2, 25.09, 25.02, 23.2, 23.1, 22.4, 19.2; HRMS (ESI) calcd for C$_{29}$H$_{50}$NO$_{10}$ [M + H]$^+$ 572.3435, found 572.3422.

(3S,3aR,5R,5aS,5bR,9aR,11S,12aS,14aR,14bS)-12a-Hydroxy-5,11,14b-tris(methoxymethoxy)-3a,8,8-trimethylhexadecahydro-6H-cyclopenta[7,8]phenanthro[4,4a-d][1,3]dioxine-3-carbonitrile (29). To a stirred solution of oxime **28** (0.300 g, 0.525 mmol) in CH$_2$Cl$_2$ (10 mL) was added 1,1′-carbonyldiimidazole (0.297 g, 1.87 mmol) at room temperature. After the mixture was stirred for 12 h, saturated aqueous NH$_4$Cl (10 mL) was added, and the mixture was extracted with CH$_2$Cl$_2$ (3 × 10 mL). The combined organic layers were dried over Na$_2$SO$_4$ and concentrated under reduced pressure to a residue, which was purified by column chromatography (silica gel, hexanes/ethyl acetate, 8:2) to furnish nitrile **29** (0.226 g, 78%) as a white foam: $[\alpha]_D^{22}$ +21.2 (c 2.15, CHCl$_3$); ^{1}H NMR (400 MHz, CDCl$_3$) δ 4.75−4.64 (m, 6H), 4.52−4.42 (m, 2H), 4.20 (q, J = 5.2 Hz, 1H), 4.07 (d, J = 17.8 Hz, 1H), 3.59 (d, J = 12.3 Hz, 1H), 3.42−3.29 (m, 9H), 3.17 (dd, J = 8.9, 7.5 Hz, 1H), 2.17−2.06 (m, 3H), 2.05−1.87 (m, 3H), 1.86−1.65 (m, 5H), 1.56−1.26 (m, 11H), 1.15 (s, 3H), 1.09−0.95 (m, 1H); ^{13}C NMR (100 MHz, CDCl$_3$) δ 120.8, 101.1, 96.3, 94.6, 92.8, 89.1, 74.8, 72.6, 70.8, 66.4, 60.7, 56.4, 56.2, 55.5, 48.2, 47.4, 44.3, 40.2, 39.2, 38.4, 35.3, 34.6, 29.5, 29.4, 27.1, 25.0, 23.1, 22.2, 20.4; HRMS (ESI) calcd for C$_{29}$H$_{48}$NO$_9$ [M + H]$^+$ 554.3329, found 554.3327.

(3S,3aR,5R,5aS,5bR,9aR,11S,12aS,14aR,14bS)-5,11,14b-Tris-(methoxymethoxy)-3a,8,8-trimethyl-3-((R)-2,2,2-trifluoro-1-hydroxyethyl)tetradecahydro-6H-cyclopenta[7,8]phenanthro[4,4a-d][1,3]dioxin-12a(1H)-ol and (3S,3aR,5R,5aS,5bR,9aR,11S,12a-S,14aR,14bS)-5,11,14b-Tris(methoxymethoxy)-3a,8,8-trimethyl-3-((S)-2,2,2-trifluoro-1-hydroxyethyl)tetradecahydro-6H-cyclopenta-[7,8]phenanthro[4,4a-d][1,3]dioxin-12a(1H)-ol (30). To a stirred solution of aldehyde **16** (0.20 g, 0.36 mmol) in THF (10 mL) were added TMSCF$_3$ (0.093 mL, 0.46 mmol, 0.5 M THF solution) and a catalytic amount (10 μL) of TBAF. After 1 h, additional TBAF (0.50 mL, 0.45 mmol, 1 M solution in THF) was added, and the mixture was stirred for 6 h at room temperature. The reaction mixture was concentrated under reduced pressure and purified by column chromatography (silica gel, hexanes/ethyl acetate, 1:1) to furnish compound **30** (0.10 g, 46%) as a white foam: $[\alpha]_D^{22}$ +24.9 (c 0.297, CHCl$_3$); ^{1}H NMR (400 MHz, CDCl$_3$) δ 4.86−4.43 (m, 8H), 4.33 (s, 1H), 4.17−4.03 (m, 2H (overlapped with EtOAc)), 3.91−3.67 (m, 1H), 3.54 (d, J = 12.2 Hz, 1H), 3.45−3.28 (m, 9H), 2.78 (td, J = 12.5, 5.5 Hz, 1H), 2.37 (dd, J = 43.6, 10.6 Hz, 1H), 2.21−1.25 (m, 20H

(overlapped with EtOAc)), 1.18−1.01 (m, 2H), 0.99−0.78 (m, 3H). HRMS (ESI) calcd for C$_{30}$H$_{50}$F$_3$O$_{10}$ [M + H]$^+$ 627.3356, found 627.3367.

(3S,3aR,5R,5aS,5bR,9aR,11S,12aS,14aR,14bS)-3-((R)-1-Hydroxy-prop-2-yn-1-yl)-5,11,14b-tris(methoxymethoxy)-3a,8,8-trimethyltetradecahydro-6H-cyclopenta[7,8]phenanthro[4,4a-d][1,3]dioxin-12a(1H)-ol and (3S,3aR,5R,5aS,5bR,9aR,11S,12aS,14aR,14bS)-3-((S)-1-Hydroxyprop-2-yn-1-yl)-5,11,14b-tris(methoxymethoxy)-3a,8,8-trimethyltetradecahydro-6H-cyclopenta[7,8]phenanthro-[4,4a-d][1,3]dioxin-12a(1H)-ol (31). To a solution of aldehyde **16** (0.170 g, 0.305 mmol) in THF (10 mL) at −78 °C was added ethynylmagnesium bromide (0.5 M solution in THF, 6.11 mL, 3.05 mmol). After stirring for 1 h, the reaction was quenched with saturated aqueous NH$_4$Cl (10 mL). The organic phase was separated, and the aqueous phase was extracted with EtOAc (2 × 15 mL). The combined organic layers were dried over Na$_2$SO$_4$ and concentrated under reduced pressure. The residue was purified by column chromatography (silica gel, hexanes/ethyl acetate, 7:3) to yield a diastereomeric mixture of alkynol **31** (0.140 g, 79%) as a white foam: $[\alpha]_D^{22}$ +11.4 (c 0.370, CHCl$_3$); ^{1}H NMR (400 MHz, CDCl$_3$) δ 4.86−4.34 (m, 8H), 4.20 (t, J = 34.7 Hz, 4H), 3.54 (dd, J = 34.2, 20.5 Hz, 2H), 3.50−3.23 (m, 9H), 2.71 (s, 1H), 2.51−2.21 (m, 2H), 2.17−1.56 (m, 8H), 1.59−1.15 (m, 12H), 1.13 (s, 1H), 0.92 (s, 3H); ^{13}C NMR (100 MHz, CDCl$_3$) δ 101.0, 96.5, 94.7, 92.8, 91.9, 86.1, 76.9, 72.6, 72.3, 71.0, 66.6, 64.1, 60.9, 56.1, 55.9, 55.5, 50.9, 47.07, 47.03, 43.0, 40.6, 38.5, 34.76, 34.40, 30.0, 29.3, 28.1, 25.1, 23.2, 21.6, 18.5; HRMS (ESI) calcd for C$_{31}$H$_{50}$O$_{10}$Na [M + Na]$^+$ 605.3302, found 605.3315.

(3S,3aR,5R,5aS,5bR,9aR,11S,12aS,14aR,14bS)-12a-Hydroxy-5,11,14b-tris(methoxymethoxy)-3a,8,8-trimethylhexadecahydro-6H-cyclopenta[7,8]phenanthro[4,4a-d][1,3]dioxine-3-carboxylic Acid (32). To a solution of hydroxyketone **14** (0.20 g, 0.34 mmol) in EtOH/H$_2$O (1:1, 10 mL) were added AcOH (1 mL) and NaIO$_4$ (0.21 g, 1.0 mmol). After stirring for 1 h, the reaction mixture was diluted with water (10 mL) and extracted with CH$_2$Cl$_2$ (3 × 10 mL). The combined organic layers were dried over Na$_2$SO$_4$ and concentrated under reduced pressure to a residue, which was purified by column chromatography (silica gel, hexanes/ethyl acetate, 6:4) to furnish acid **32** (0.10 g, 52%) as a white foam: $[\alpha]_D^{22}$ −5.47 (c 1.09, CHCl$_3$); ^{1}H NMR (400 MHz, CDCl$_3$) δ 4.84 (d, J = 6.8 Hz, 1H), 4.81−4.67 (m, 3H), 4.59 (t, J = 4.4 Hz, 3H), 4.55−4.36 (m, 3H), 4.12 (s, 1H), 3.57 (t, J = 10.6 Hz, 1H), 3.45 (dt, J = 17.0, 8.5 Hz, 1H), 3.42−3.31 (m, 9H), 2.28−2.02 (m, 4H), 1.96 (dd, J = 14.8, 3.1 Hz, 1H), 1.84 (dt, J = 18.2, 9.5 Hz, 4H), 1.66 (ddd, J = 26.9, 16.7, 9.5 Hz, 1H), 1.58−1.26 (m, 11H), 1.20−1.01 (m, 1H), 0.86 (s, 3H); ^{13}C NMR (100 MHz, CDCl$_3$) δ 177.8, 101.1, 95.1, 94.6, 92.8, 90.4, 73.9, 72.6, 70.9, 66.3, 60.8, 56.3, 56.1, 55.6, 51.2, 47.4, 47.0, 43.4, 40.9, 36.1, 34.8, 34.4, 29.6, 29.4, 25.9, 25.1, 23.2, 21.8, 20.6; HRMS (ESI) calcd for C$_{29}$H$_{49}$O$_{11}$ [M + H]$^+$ 573.3275, found 573.3257.

Insect Cells and Viral Infections. All four isoforms of Na,K-ATPase were expressed in Sf9 cells. They were grown in Grace's medium (JRH Biosciences, Lenexa, KS, USA) with 3.3 g/L of lactalbumin hydrolysate and 3.3 g/L of yeastolate and supplemented with 10% (v/v) fetal bovine serum, 100 units/mL of penicillin, 100 μg/mL of streptomycin, and 0.25 μg/mLof fungizone. Infections were performed in 150 mm Petri dishes as previously described.[74] After 72 h at 27 °C, cells were scraped from the culture plates, centrifuged at 1500× g for 10 min, and washed twice in 10 mM imidazole hydrochloride (pH 7.5) and 1 mM EGTA. Cells were then suspended in the same solution homogenized as described and used for assays.[35]

Na,K-ATPase Assay. Na,K-ATPase activity was assayed for all four isoforms using insect cells homogenates. Na,K-ATPase activity was determined by the initial rate of release of ^{32}P$_i$ from $\gamma[^{32}$P]-ATP as described.[35,74] The incubation medium (0.25 mL) contained 120 mM NaCl, 30 mM KCl, 3 mM MgCl$_2$, 0.2 mM EGTA, 30 mM Tris-HCl (pH 7.4), and different concentrations of ouabain analogues. The assay was started by the addition of ATP with 0.2 μCi $\gamma[^{32}$P]-ATP (at a final concentration of 2 mM). After 30 min of incubation at 37 °C, the ^{32}P$_i$ released by the Na,K-ATPase reaction was complexed to molybdate in acidic medium by adding 5% ammonium molybdate in 4 N H$_2$SO$_4$. The resulting phosphomolybdate was extracted with isobutanol as described.[75] Radioactivity in 170 μL of the organic phase was

measured by liquid scintillation counting. Enzymatic activity was determined as the difference in ATP hydrolysis in the absence and presence of 1 mM ouabain.

Rat Sperm Preparations. All experimental protocols involving animals used in this work were approved by the University of Kansas Medical Center Institutional Animal Care and Use Committee. Long Evans rats were purchased from Harlan (Indianapolis, IN). Spermatozoa were obtained from the cauda of adult rat epididymis, in modified Tyrode's medium, containing 95 mM NaCl, 4.7 mM KCl, 1.2 mM KH_2PO_4, 1.2 mM $MgSO_4$, 5.5 mM glucose, 0.27 mM pyruvic acid, 0.25 mM lactic acid, 40 mM Hepes, and 20 mM Tris, as previously described.[32]

In Vivo Testing of Compounds. Compound **25** was administered to rats by oral gavage. Two protocols were used; in one, male rats were treated with 5, 10, and 20 mg/kg of compound **25** daily for a total of 3 days. In the other, a daily dose of 5 mg/kg weight was given for 3, 6, 9, or 12 days. After treatment, animals were sacrificed; sperm was collected from the cauda epididymis, and sperm motility was measured by CASA.

Sperm Motility Assays. Approximately 3×10^6 cells were incubated in 300 μL of the modified Tyrode's medium, with the addition of 1.7 mM $CaCl_2$, and in the absence and presence of different amounts of the ouabain analogues for 60 min. Incubation was performed at 37 °C. Then, cells were labeled with 2 μL of a 75 μM stock of the green fluorescent nucleic acid stain SYTO 21, which allows tracking of cell movement. After 2 min of incubation with the dye, 7 μL aliquots from each sample were taken and placed into a glass cell chamber (Leja Products B.V., The Netherlands). Sperm motility was determined as described before.[32] Briefly, cells were viewed with an Olympus BX51 microscope through a 20× phase objective and maintained at 37 °C on a heated platform. Viewing areas on each chamber were captured using a CCD camera. Samples were analyzed by CASA using the Minitube SpermVision Digital Semen Evaluation system (version 3.5; Penetrating Innovations, Verona, WI, USA). An average of 200 cells/field were captured, at a rate of 30 frames per field and, a total of 10 fields in each sample were analyzed. Different sperm motility parameters were analyzed, including total motility, progressive motility, curvilinear, average path, and straight line velocities, amplitude of lateral head displacement, beat cross frequency, and linearity. The analytical setup parameters used were those published previously.[33] To assess the hyperactive pattern of motility, typical of sperm capacitation, cells were incubated in modified Tyrode's medium with the addition of 1.7 mM $CaCl_2$, 25 mM sodium bicarbonate, and 0.5% bovine serum albumin.[33] Experiments were performed in triplicate, and values expressed as the mean $\pm$ SEM.

Membrane Potential Measurements. Membrane potential was determined using the fluorescent indicator $[DiSC_3(5)]$ as described.[76,77] Sperm samples containing 2×10^6 cells/mL were treated with modified Tyrode's medium for 20 min at 37 °C with and without compound **25** in a concentration of 10^{-8} M.[31] Then, $[DiSC_3(5)]$, at a final concentration of 1 μM, was added, and the samples were incubated at 37 °C for an additional 8 min. Sperm were further incubated for another 2 min with carbonyl cyanide *m*-chlorophenylhydrazone (CCCP) at a final concentration of 1 μM, to avoid interference of the mitochondrial membrane potential as described.[78] After this time period, 2.5 mL of the suspension were transferred into a cuvette arranged with gentle stirring and maintained at 37 °C, and fluorescence at an excitation/emission wavelength of 620/670 nm was recorded. Calibration of the fluorescence changes into millivolts was done in the same sample by adjusting the membrane potential of the cells as described previously using the K^+ ionophore, valinomycin, and stepwise addition of K^+.[77] Membrane potential was calculated after distribution of K^+ between the medium and the cells, which follows the Nernst equilibrium. Values were obtained by interpolation using the plasma membrane potential versus arbitrary units of fluorescence as described previously.[77]

Intracellular pH Measurements. Sperm intracellular pH was measured with the pH-sensitive dye SNARF-1-AM as described.[32] Spermatozoa (20×10^6 cells/mL) were incubated in modified Tyrode's medium adjusted at different pH values (7.0, 7.2, 7.4, and

7.6) for 15 min at 37 °C in the absence or presence of 10^{-3} M compound **25**. Then, the cell-permeable nonfluorescent precursor SNARF-1-AM at a concentration of 5 μM was added, and the cells were incubated for another 30 min at 37 °C. After centrifugation at 300 g for 5 min, the cells were resuspended in 100 μL of fresh modified Tyrode's medium, and 15 μL aliquots were transferred to cuvettes with a total volume of 2.5 mL of modified Tyrode's medium. Calibrating controls consisted in sperm resuspended in medium at preset pH values (6.0, 7.0, 7.2, 7.4, 7.6, and 8.0) and treated with 2 μg/mL of the ionophore nigericin for 20 min to permeabilize the cells and clamp the intracellular pH.[79] Fluorescence was measured at an excitation of 488 nm and at an emission ratio of 640/580 nm, and cell pH was calculated based on the pH-dependent spectral shift of SNARF-1.

Intracellular Ca^{2+} Determination. Changes in $[Ca^{2+}]_i$ were determined using the cell-permeable fluorescent dye Calcium Green-1-AM.[80] Cells in modified Tyrode's medium without Ca^{2+} were treated without and with 10^{-8} M compound **25**. Spermatozoa were loaded with Calcium Green-1-AM, used at a final concentration of 5 μM. After washing the cells twice in modified Tyrode's medium and centrifugation at 300 g for 5 min, the cells were resuspended in fresh medium and placed on slides. Cells were then subjected to confocal microscopy. Cell fluorescence of individual cells were viewed by confocal microscopy at an excitation/emission of 488/515−530 nm. Images were collected using a Nikon scope and a 20× objective. The samples were maintained at 37 °C, employing a heated device regulated by the system acquisition control. Analysis of the collected data was done using Metamorph software (Molecular Devices, Downingtown, PA, USA). A total of 60 cells per experimental condition were analyzed in each experiment, and the results were expressed relative to the control, in which ouabain was omitted.

General Metabolic Stability Permeability and Toxicity Assays. ADMET studies were performed for compound **25** at Cerep (Seattle, WA). S9Metabolic stability was assessed in microsomal liver samples from human, monkey, dog, rat, and mouse hepatocytes.

In vitro absorption of the compound was tested in vitro by assessing the passage of compound across monolayers of human colon carcinoma cells (Caco-2 cells) grown on Transwell tissue culture plates. Recovery of the test compounds to the side, opposite to the place where they were added, and the apparent permeability coefficient for each compound were determined. Conditions: A-to-B flux at 37 °C with shaking; 96-well Multiscreen plate; pH 6.5 in A and pH 7.4 in B. Donor samples: 0−60 min. Receiver sample 60 min. B-to-A flux at 37 °C with shaking; 96-well Multiscreen plate; pH 6.5 in A and pH 7.4 in B. Donor samples: 0−40 min. Receiver sample: 40 min. The compound was identified by full scan HPLC-MS. Total ion current chromatograms and the corresponding mass spectra were generated for the compound in both positive and negative ionization modes.

To gain insight on potential toxicity of compound **25**, two basic tests were used. One consisted of the effect of **25** on human ether-a-go-go-related gene (hERG) tail current recorded from human embryonic kidney (HEK293) cells stably transfected with hERG cDNA. The other assay was the antiproliferative assay in MCF-7 cells, which follows proliferation and viability of cells after administration of increasing concentrations of the tested compounds.

Homology Modeling of Na,K-ATPase Isoforms. The sequences of the rat Na,K-ATPase isoforms were obtained from the uniprot database.[81,82] The most relevant for this study were the shark-derived Na,K-ATPase in the ouabain-bound state (PDB ID: 3A3Y) and the shark-derived apo Na,K-ATPase (PDB ID: 2ZXE).[45] To facilitate building structural models of the Na,K-ATPase isoforms, protein sequence alignments of the sequences of the Na,K-ATPase isoforms with available template structure of Na,K-ATPase (3A3Y) were performed using Prime.[51] The initial models were constructed in Prime.[51] The models of the Na,K-ATPase isoforms were relaxed with MacroModel using OPLS2005 force field until converging at a termination gradient of 0.05 kJ/mol Å.[53] Ouabain was incorporated into each relaxed model of Na,K-ATPase isoforms. Finally, the crude model structures from Prime were refined using Protein Preparation Wizard (Schrodinger Suite 2009) in Maestro.[51,54,83,84]

General Procedure of Molecular Docking and Relative Binding (Free) Energy Calculations. Homology model structures of the rat Na,K-ATPase $\alpha 1$ and $\alpha 4$, refined using the Protein Preparation Wizard in Maestro,[51,84] were used to generate receptor grids using Glide.[85] Grid centroids of the homology model structures were established by selecting amino acid residues that define the binding site (Ile322, Ile328, Val329, Ala330, and Thr804). The limit of the ligand length was ≤ 36 Å, and the grid dimension was 14 Å $\times$ 10 Å $\times$ 14 Å in all cases. LigPrep was used to prepare ligands for docking simulations.[86] A series of docking simulations (HTVS, SP, and XP modes) were performed in Glide.[85] Docking poses obtained from XP docking simulations were used for relative binding free energy calculation using MM-GBSA method in Prime.[51] Input ligand partial charges were used, and the flexible residue distance was defined as 5 Å from the ligand in the MM-GBSA calculation.

Energy Minimization. Energy minimizations of the structures of proteins or the complexes of proteins with ligands were performed in MacroModel using OPLS2005 force field. The minimization was set up to stop at the threshold gradient of 0.05 kJ/mol Å with a Polak-Ribiere Conjugate Gradient (PRCG) method.

Molecular Dynamics Simulation. The complexes of the rat $\alpha 1$ and $\alpha 4$ isoforms of Na,K-ATPase with ligands were taken for the generation of the system files for the MD simulation. The simulation boxes with TIP4P solvent molecules were generated with the dimension of 10 Å $\times$ 10 Å $\times$ 10 Å using OPLS2005 force-field in desmond.[55] The model systems were neutralized by adding Na$^+$ ions: 21 Na$^+$ for the rat $\alpha 1$ and 16 Na$^+$ for the rat $\alpha 4$. Membranes were incorporated to the transmembrane domains of the complexes of the enzymes and the ligands based on information from OPM database (opm.phar.umich.edu, PDB ID: 3A3Y) and uniprot database. Following the generation of model systems for MD simulations, the initial short time scale MD simulation (1.2 ps) with 1.2 fs time step was performed using the desmond graphics user interface (desmond GUI).[55] After that, 18 ns MD simulations of the complexes were performed using desmond 3.0 employing 128 cores in a high-performance computing system. Default option in desmond/2011 for integration, ensemble, interaction, restraints, output, and Misc were used except Thermostat and Barostat methods in Ensemble; Berendsen method was used as Thermostat and Barostat methods with relaxation time of 1.0 ps and isotropic coupling style for the barostat.[85]

Data Analysis. Statistical significance of the differences between the effect of the compounds, depending on dose, time of action, and isoform selectivity was determined by ANOVA, followed by Tukey's post-test for multiple comparisons. Statistical significance was defined as $P < 0.05$. Comparisons of the effect of the compounds on sperm membrane potential, intracellular pH, and $[Ca^{2+}]_i$ was assessed by Student's t test.

ASSOCIATED CONTENT

Ⓢ Supporting Information

The Supporting Information is available free of charge on the ACS Publications website at DOI: 10.1021/acs.jmedchem.7b00925.

> ^{1}H and ^{13}C NMR spectra of all new compounds, supplementary computational information, antiproliferative assay data, hERG data, and data for reference compounds for Caco-2 in vitro absorption assay (PDF)
> Molecular formula strings (CSV)
> Hydrogen-suppressed homology models of the rat Na,K-ATPase $\alpha 1$ (PDB)
> Hydrogen-suppressed homology models of the rat Na,K-ATPase $\alpha 4$ (PDB)

AUTHOR INFORMATION

Corresponding Authors
*E-mail: georg@umn.edu. Phone: (612) 626-5329.

*E-mail: gblanco@kumc.edu. Phone: (913) 588-7405.

ORCID ⦿
Gunda I. Georg: 0000-0002-8900-9460

Notes
The authors declare no competing financial interest.

ABBREVIATIONS USED

BLQ, below the limit of quantitation; Caco-2, human epithelial colorectal adenocarcinoma cells; Calcium Green-1-AM, glycine, N-[2-[(acetyloxy)methoxy]-2-oxoethyl]-N-[2-[2-[5-[[[3′,6′-bis(acetyloxy)-2′,7′-dichloro-3-oxospiro[isobenzofuran-1-(3H),9′-[9H]xanthen]-5-yl]carbonyl]amino]-2-[bis[2-[(acetyloxy)methoxy]-2-oxoethyl]amino]phenoxy]ethoxy]-phenyl]-(acetyloxy)methyl ester; CASA, computer-assisted sperm analysis; CCD, charge coupled device camera; CCCP, carbonyl cyanide m-chlorophenylhydrazone; CDI, carbon-yldiimidazole; DIPEA, N,N-diisopropylethylamine; DiSC3(5), 3,3′-dipropylthiadicarbocyanine iodide; EGTA, ethylene glycol-bis(β-aminoethyl ether)-N,N,N′,N′-tetraacetic acid; E_m, membrane potential; hERG, human ether-a-go-go-related gene; HEK293, human embryonic kidney 293 cells; MCF-7, Michigan Cancer Foundation-7 human breast cancer cell line; MOM-Cl, methoxymethyl chloride; Sf9 cells, clonal isolate from *Spodoptera frugiperda* Sf21 cells; SYTO 21, green fluorescent nucleic acid stain 21; SNARF-1-AM, fluorescein/carboxy-seminaphtharhodafluor-1-(acetyloxy)methyl ester; TMSCF$_3$, trifluoromethyltrimethylsilane; TsCl, 4-toluenesulfonyl chloride; WHO, World Health Organization

REFERENCES

(1) Pickle, S.; Wu, J.; Burbank-Schmitt, E. Prevention of unintended pregnancy: a focus on long-acting reversible contraception. *Prim. Care* **2014**, *41*, 239−260.

(2) Cornet, A. Current challenges in contraception in adolescents and young women. *Curr. Opin. Obstet. Gynecol.* **2013**, *25*, S1−S10.

(3) Cheng, C. Y.; Mruk, D. D. New frontiers in nonhormonal male contraception. *Contraception* **2010**, *82*, 476−482.

(4) Frank, P. I.; Kay, C. R.; Scott, L. M.; Hannaford, P. C.; Haran, D. Pregnancy following induced abortion: maternal morbidity, congenital abnormalities and neonatal death. Royal College of General Practitioners/Royal College of Obstetricians and Gynaecologists Joint Study. *BJOG* **1987**, *94*, 836−842.

(5) Michie, L.; Cameron, S. T. Improving the uptake of long acting reversible contraception: a review. *Minerva Ginecol.* **2013**, *65*, 241−252.

(6) Bitzer, J.; Simon, J. A. Current issues and available options in combined hormonal contraception. *Contraception* **2011**, *84*, 342−356.

(7) Wiegratz, I.; Thaler, C. J. Hormonal contraception—what kind, when, and for whom? *Dtsch. Ärzteb. Int.* **2011**, *108*, 495−505; quiz 506.

(8) Sitruk-Ware, R. Contraception: an international perspective. *Contraception* **2006**, *73*, 215−222.

(9) Payne, C.; Goldberg, E. Male contraception: past, present and future. *Curr. Mol. Pharmacol.* **2015**, *7*, 175−181.

(10) Heinemann, K.; Saad, F.; Wiesemes, M.; White, S.; Heinemann, L. Attitudes toward male fertility control: results of a multinational survey on four continents. *Hum. Reprod.* **2005**, *20*, 549−556.

(11) Dorman, E.; Bishai, D. Demand for male contraception. *Expert Rev. Pharmacoecon. Outcomes Res.* **2012**, *12*, 605−613.

(12) Jensen, J. T. Why family planning matters. *Rev. Endocr. Metab. Disord.* **2011**, *12*, 55−62.

(13) Lishko, P. V.; Kirichok, Y.; Ren, D.; Navarro, B.; Chung, J. J.; Clapham, D. E. The control of male fertility by spermatozoan ion channels. *Annu. Rev. Physiol.* **2012**, *74*, 453−475.

(14) Zheng, L. P.; Wang, H. F.; Li, B. M.; Zeng, X. H. Sperm-specific ion channels: targets holding the most potential for male contraceptives in development. *Contraception* **2013**, *88*, 485−491.

(15) Singh, A. P.; Rajender, S. CatSper channel, sperm function and male fertility. *Reprod. BioMed. Online* **2015**, *30*, 28−38.

(16) Visconti, P. E.; Krapf, D.; de la Vega-Beltran, J. L.; Acevedo, J. J.; Darszon, A. Ion channels, phosphorylation and mammalian sperm capacitation. *Asian J. Androl.* **2011**, *13*, 395−405.

(17) Shukla, K. K.; Mahdi, A. A.; Rajender, S. Ion channels in sperm physiology and male fertility and infertility. *J. Androl.* **2012**, *33*, 777−788.

(18) Navarro, B.; Kirichok, Y.; Chung, J. J.; Clapham, D. E. Ion channels that control fertility in mammalian spermatozoa. *Int. J. Dev. Biol.* **2008**, *52*, 607−613.

(19) Jimenez, T.; McDermott, J. P.; Sanchez, G.; Blanco, G. Na,K-ATPase alpha4 isoform is essential for sperm fertility. *Proc. Natl. Acad. Sci. U. S. A.* **2011**, *108*, 644−649.

(20) McDermott, J.; Sanchez, G.; Nangia, A. K.; Blanco, G. Role of human Na,K-ATPase alpha 4 in sperm function, derived from studies in transgenic mice. *Mol. Reprod. Dev.* **2015**, *82*, 167−181.

(21) Clarke, R. J.; Fan, X. Pumping ions. *Clin. Exp. Pharmacol. Physiol.* **2011**, *38*, 726−733.

(22) Kaplan, J. H. Biochemistry of Na,K-ATPase. *Annu. Rev. Biochem.* **2002**, *71*, 511−535.

(23) Morth, J. P.; Pedersen, B. P.; Buch-Pedersen, M. J.; Andersen, J. P.; Vilsen, B.; Palmgren, M. G.; Nissen, P. A structural overview of the plasma membrane Na+,K+-ATPase and H+-ATPase ion pumps. *Nat. Rev. Mol. Cell Biol.* **2011**, *12*, 60−70.

(24) Geering, K. Functional roles of Na,K-ATPase subunits. *Curr. Opin. Nephrol. Hypertens.* **2008**, *17*, 526−532.

(25) Blanco, G. Na,K-ATPase subunit heterogeneity as a mechanism for tissue-specific ion regulation. *Semin. Nephrol.* **2005**, *25*, 292−303.

(26) Lingrel, J. B. Na,K-ATPase: isoform structure, function, and expression. *J. Bioenerg. Biomembr.* **1992**, *24*, 263−270.

(27) Mobasheri, A.; Avila, J.; Cozar-Castellano, I.; Brownleader, M. D.; Trevan, M.; Francis, M. J.; Lamb, J. F.; Martin-Vasallo, P. Na+, K +-ATPase isozyme diversity; comparative biochemistry and physiological implications of novel functional interactions. *Biosci. Rep.* **2000**, *20*, 51−91.

(28) Blanco, G.; Mercer, R. W. Isozymes of the Na-K-ATPase: heterogeneity in structure, diversity in function. *Am. J. Physiol.* **1998**, *275*, F633−F650.

(29) Blanco, G.; Sanchez, G.; Melton, R. J.; Tourtellotte, W. G.; Mercer, R. W. The alpha4 isoform of the Na,K-ATPase is expressed in the germ cells of the testes. *J. Histochem. Cytochem.* **2000**, *48*, 1023−1032.

(30) McDermott, J. P.; Sanchez, G.; Chennathukuzhi, V.; Blanco, G. Green fluorescence protein driven by the Na,K-ATPase alpha4 isoform promoter is expressed only in male germ cells of mouse testis. *J. Assist. Reprod. Genet.* **2012**, *29*, 1313−1325.

(31) Wagoner, K.; Sanchez, G.; Nguyen, A. N.; Enders, G. C.; Blanco, G. Different expression and activity of the alpha1 and alpha4 isoforms of the Na,K-ATPase during rat male germ cell ontogeny. *Reproduction* **2005**, *130*, 627−641.

(32) Jimenez, T.; Sanchez, G.; Wertheimer, E.; Blanco, G. Activity of the Na,K-ATPase α4 isoform is important for membrane potential, intracellular Ca2+, and pH to maintain motility in rat spermatozoa. *Reproduction* **2010**, *139*, 835−845.

(33) Jimenez, T.; Sanchez, G.; Blanco, G. Activity of the Na,K-ATPase alpha4 isoform is regulated during sperm capacitation to support sperm motility. *J. Androl.* **2012**, *33*, 1047−1057.

(34) Woo, A. L.; James, P. F.; Lingrel, J. B. Sperm motility is dependent on a unique isoform of the Na,K-ATPase. *J. Biol. Chem.* **2000**, *275*, 20693−20699.

(35) Blanco, G.; Melton, R. J.; Sanchez, G.; Mercer, R. W. Functional characterization of a testes-specific α-subunit isoform of the sodium/potassium adenosinetriphosphatase. *Biochemistry* **1999**, *38*, 13661−13669.

(36) Voldsgaard Clausen, M.; Nissen, P.; Poulsen, H. The α4 isoform of the Na+,K+-ATPase is tuned for changing extracellular environments. *FEBS J.* **2016**, *283*, 282−293.

(37) Fuerstenwerth, H. Ouabain - the insulin of the heart. *Int. J. Clin. Pract.* **2010**, *64*, 1591−1594.

(38) Schoner, W.; Scheiner-Bobis, G. Endogenous cardiac glycosides: hormones using the sodium pump as signal transducer. *Semin. Nephrol.* **2005**, *25*, 343−351.

(39) Schoner, W. Endogenous cardiac glycosides, a new class of steroid hormones. *Eur. J. Biochem.* **2002**, *269*, 2440−2448.

(40) Sanchez, G.; Nguyen, A. N.; Timmerberg, B.; Tash, J. S.; Blanco, G. The Na,K-ATPase α4 isoform from humans has distinct enzymatic properties and is important for sperm motility. *Mol. Hum. Reprod.* **2006**, *12*, 565−576.

(41) Yang, Y.; Wan, Y.; Lou, H.; Xue, T.; Su, P. Relationship between ouabain and asthenozoospermia. *J. Huazhong Univ. Sci. Technol., Med. Sci.* **2014**, *34*, 87−90.

(42) Blanco, G.; Hatfield, W. R.; Minor, N. T.; Sanchez, G.; Koster, J. C.; DeTomaso, A. W.; Mercer, R. W. Studies of Na,K-ATPase structure and function using baculovirus. *Ann. N. Y. Acad. Sci.* **1997**, *834*, 88−96.

(43) Koster, J. C.; Blanco, G.; Mills, P. B.; Mercer, R. W. Substitutions of glutamate 781 in the Na,K-ATPase alpha subunit demonstrate reduced cation selectivity and an increased affinity for ATP. *J. Biol. Chem.* **1996**, *271*, 2413−2421.

(44) Gupta, S. P. Quantitative structure-activity relationship studies on Na+,K+-ATPase inhibitors. *Chem. Rev.* **2012**, *112*, 3171−3192.

(45) Ogawa, H.; Shinoda, T.; Cornelius, F.; Toyoshima, C. Crystal structure of the sodium-potassium pump (Na+,K+-ATPase) with bound potassium and ouabain. *Proc. Natl. Acad. Sci. U. S. A.* **2009**, *106*, 13742−13747.

(46) Imperio, D.; Pirali, T.; Galli, U.; Pagliai, F.; Cafici, L.; Canonico, P. L.; Sorba, G.; Genazzani, A. A.; Tron, G. C. Replacement of the lactone moiety on podophyllotoxin and steganacin analogues with a 1,5-disubstituted 1,2,3-triazole via ruthenium-catalyzed click chemistry. *Bioorg. Med. Chem.* **2007**, *15*, 6748−6757.

(47) McClure, K. F.; Abramov, Y. A.; Laird, E. R.; Barberia, J. T.; Cai, W.; Carty, T. J.; Cortina, S. R.; Danley, D. E.; Dipesa, A. J.; Donahue, K. M.; Dombroski, M. A.; Elliott, N. C.; Gabel, C. A.; Han, S.; Hynes, T. R.; Lemotte, P. K.; Mansour, M. N.; Marr, E. S.; Letavic, M. A.; Pandit, J.; Ripin, D. B.; Sweeney, F. J.; Tan, D.; Tao, Y. Theoretical and experimental design of atypical kinase inhibitors: application to p38 MAP kinase. *J. Med. Chem.* **2005**, *48*, 5728−5737.

(48) Hong, B.-C.; Kim, S.; Kim, T.-S.; Corey, E. J. Synthesis and properties of several isomers of the cardioactive steroid ouabain. *Tetrahedron Lett.* **2006**, *47*, 2711−2715.

(49) Sneeden, R. P. A.; Turner, R. B.; Ouabagenin, I. The relationship between ouabagenin monoacetonide and "anhydroouabagenin". *J. Am. Chem. Soc.* **1953**, *75*, 3510−3513.

(50) Renata, H.; Zhou, Q.; Dunstl, G.; Felding, J.; Merchant, R. R.; Yeh, C.-H.; Baran, P. S. Development of a concise synthesis of ouabagenin and hydroxylated corticosteroid analogues. *J. Am. Chem. Soc.* **2015**, *137*, 1330−1340.

(51) *Prime*, version 3.1; Schrodinger, LLC: New York, NY, 2012.

(52) Morth, J. P.; Pedersen, B. P.; Toustrup-Jensen, M. S.; Soerensen, T. L. M.; Petersen, J.; Andersen, J. P.; Vilsen, B.; Nissen, P. Crystal structure of the sodium-potassium pump. *Nature* **2007**, *450*, 1043−1049.

(53) *MacroModel*, version 9.9; Schrodinger, LLC: New York, NY, 2012.

(54) *Protein Preparation Wizard*; Schrodinger, LLC: New York, NY, 2012.

(55) (a) *Desmond Molecular Dynamics System*, version 3.0; D. E. Shaw Research: New York, NY, 2011. (b) *Maestro-Desmond Interoperability Tools*, version 3.0; Schrodinger: New York, NY, 2011.

(56) Feng, J.; Lingrel, J. B. Analysis of amino acid residues in the H5-H6 transmembrane and extracellular domains of Na,K-ATPase α subunit identifies threonine 797 as a determinant of ouabain sensitivity. *Biochemistry* **1994**, *33*, 4218–4224.

(57) Suarez, S. S.; Ho, H. C. Hyperactivation of mammalian sperm. *Cell. Mol. Biol.* **2003**, *49*, 351–356.

(58) Ickowicz, D.; Finkelstein, M.; Breitbart, H. Mechanism of sperm capacitation and the acrosome reaction: role of protein kinases. *Asian J. Androl.* **2012**, *14*, 816–821.

(59) Ikawa, M.; Inoue, N.; Benham, A. M.; Okabe, M. Fertilization: a sperm's journey to and interaction with the oocyte. *J. Clin. Invest.* **2010**, *120*, 984–994.

(60) Darszon, A.; Trevino, C. L.; Wood, C.; Galindo, B.; Rodriguez-Miranda, E.; Acevedo, J. J.; Hernandez-Gonzalez, E. O.; Beltran, C.; Martinez-Lopez, P.; Nishigaki, T. Ion channels in sperm motility and capacitation. *Soc. Reprod. Fertil. Suppl.* **2007**, *65*, 229–244.

(61) Buffone, M. G.; Ijiri, T. W.; Cao, W.; Merdiushev, T.; Aghajanian, H. K.; Gerton, G. L. Heads or tails? Structural events and molecular mechanisms that promote mammalian sperm acrosomal exocytosis and motility. *Mol. Reprod. Dev.* **2012**, *79*, 4–18.

(62) Cooper, T. G.; Noonan, E.; von Eckardstein, S.; Auger, J.; Baker, H. W.; Behre, H. M.; Haugen, T. B.; Kruger, T.; Wang, C.; Mbizvo, M. T.; Vogelsong, K. M. World Health Organization reference values for human semen characteristics. *Hum. Reprod. Update* **2010**, *16*, 231–245.

(63) Okabe, M. The cell biology of mammalian fertilization. *Development* **2013**, *140*, 4471–4479.

(64) Harayama, H. Roles of intracellular cyclic AMP signal transduction in the capacitation and subsequent hyperactivation of mouse and boar spermatozoa. *J. Reprod. Dev.* **2013**, *59*, 421–430.

(65) Suarez, S. S. Control of hyperactivation in sperm. *Hum. Reprod. Update* **2008**, *14*, 647–657.

(66) Slott, V. L.; Suarez, J. D.; Perreault, S. D. Rat sperm motility analysis: methodologic considerations. *Reprod. Toxicol.* **1991**, *5*, 449–458.

(67) Daut, J. Inhibition of the sodium pump in guinea-pig ventricular muscle by dihydro-ouabain: effects of external potassium and sodium. *J. Physiol.* **1983**, *339*, 643–662.

(68) Crambert, G.; Hasler, U.; Beggah, A. T.; Yu, C.; Modyanov, N. N.; Horisberger, J. D.; Lelievre, L.; Geering, K. Transport and pharmacological properties of nine different human Na, K-ATPase isozymes. *J. Biol. Chem.* **2000**, *275*, 1976–1986.

(69) Brown, L.; Erdmann, E. Binding of digitalis derivatives to beef, cat and human cardiac (Na+ + K+)-ATPase. Affinity and kinetic constants. *Arch. Int. Pharmacodyn. Ther.* **1984**, *271*, 229–240.

(70) O'Brien, W. J.; Lingrel, J. B.; Wallick, E. T. Ouabain binding kinetics of the rat alpha two and alpha three isoforms of the sodium-potassium adenosine triphosphate. *Arch. Biochem. Biophys.* **1994**, *310*, 32–39.

(71) Mruk, D. D.; Cheng, C. Y. The mammalian blood-testis barrier: its biology and regulation. *Endocr. Rev.* **2015**, *36*, 564–591.

(72) Gregory, M.; Cyr, D. G. The blood-epididymis barrier and inflammation. *Spermatogenesis* **2014**, *4*, e979619.

(73) Mital, P.; Hinton, B. T.; Dufour, J. M. The blood-testis and blood-epididymis barriers are more than just their tight junctions. *Biol. Reprod.* **2011**, *84*, 851–858.

(74) Blanco, G.; Sanchez, G.; Mercer, R. W. Comparison of the enzymatic properties of the Na,K-ATPase $\alpha 3\beta 1$ and $\alpha 3\beta 2$ isozymes. *Biochemistry* **1995**, *34*, 9897–9903.

(75) Beauge, L.; Campos, M. A. Calcium inhibition of the atpase and phosphatase activities of (Na+ + K+)-ATPase. *Biochim. Biophys. Acta, Biomembr.* **1983**, *729*, 137–149.

(76) Plasek, J.; Hrouda, V. Assessment of membrane potential changes using the carbocyanine dye, diS-C3-(5): synchronous excitation spectroscopy studies. *Eur. Biophys. J.* **1991**, *19*, 183–188.

(77) Espinosa, F.; Darszon, A. Mouse sperm membrane potential: changes induced by Ca2+. *FEBS Lett.* **1995**, *372*, 119–125.

(78) Hernandez-Gonzalez, E. O.; Sosnik, J.; Edwards, J.; Acevedo, J. J.; Mendoza-Lujambio, I.; Lopez-Gonzalez, I.; Demarco, I.; Wertheimer, E.; Darszon, A.; Visconti, P. E. Sodium and epithelial sodium channels participate in the regulation of the capacitation-associated hyperpolarization in mouse sperm. *J. Biol. Chem.* **2006**, *281*, 5623–5633.

(79) Chow, S.; Hedley, D. Flow cytometric measurement of intracellular pH. *Curr. Protoc. Cytom.* **2001**.

(80) June, C. H.; Abe, R.; Rabinovitch, P. S. Measurement of intracellular calcium ions by flow cytometry. *Curr. Protoc. Cytom.* **2001**.

(81) Shamraj, O. I.; Lingrel, J. B. A putative fourth Na+,K+-ATPase α-subunit gene is expressed in testis. *Proc. Natl. Acad. Sci. U. S. A.* **1994**, *91*, 12952–12956.

(82) Hlivko, J. T.; Chakraborty, S.; Hlivko, T. J.; Sengupta, A.; James, P. F. The human Na,K-ATPase alpha4 isoform is a ouabain-sensitive alpha isoform that is expressed in sperm. *Mol. Reprod. Dev.* **2006**, *73*, 101–115.

(83) *Impact*, version 5.8; Schrodinger, LLC: New York, NY, 2012.

(84) *Epik*, version 2.3; Schrodinger, LLC: New York, NY, 2012.

(85) *Glide*, version 5.8; Schrodinger, LLC: New York, NY, 2012.

(86) *LigPrep*, version 2.5; Schrodinger, LLC: New York, NY, 2012.